Replies to Reviewer #2 Comments/Suggestions

This paper deals with the trends and variabilities of Asian Summer Monsoon anticyclone (ASMA) using observational and reanalysis datasets. It deals with the spatial and temporal variabilities of ASMA and its relationship with long term oscillations. The subject dealt with is a very active and relevant topic. However, as I have already pointed out in my initial review, the methodology used for the study and structure of the manuscript needs major revisions.

Reply: First of all we wish to thank the reviewer for handling this manuscript and for offering his/her constructive comments/suggestions, which improved the manuscript content significantly. In the revised version, we have taken care of the reviewers comments/suggestions and we hope the reviewer will find the revised version satisfactory. As per reviewer suggestion, the methodology part and structure of the manuscript is changed according to results.

(1) The authors must bring out the novelty of the study properly. Throughout the manuscript, the already known facts and the results of the present study are in a completely messed up state, for example in the abstract itself. The authors have stated the known facts of ASMA in the abstract. The abstract should focus on the major results of the present study.

Reply: As per reviewer suggestion, we have removed the basic introduction part from the abstract and focused on the mentioning major results of the study.

(2) In the trend analysis, the relevance of dividing the ASMA region into four different sectors is not clear.

Reply: In the revised version, we have given following reason for dividing the ASMA into 4 different regions.
The spatial trend analysis of ASMA shows distinct variability throughout the region and the edges of the ASMA undergo drastic variability compared to other regions. Therefore, in order to understand the asymmetry in the anticyclone variability, we have divided the anticyclone region into 4 different sectors as shown in Figure 4 based on the peak values of GPH along longitude and latitude cross-sections.

(3) What is the sanctity in averaging the wind, when the wind magnitudes are highly inhomogeneous (calm wind near to the centre of ASMA and higher wind to the edges) in all these sectors? Spatial extent of ASMA is discussed in the manuscript. No mention about the altitude/vertical extent of ASMA. This needs to be discussed.

Reply: As mentioned above, depending upon the spatial variability of ASMA, we have divided into 4 different sectors. In order to verify the zonal wind variability in ASMA region, we have selected 3 different locations in Figure R1. At these locations also the zonal wind anomalies shows significant increasing trend similar to the variability in four different sectors.

Figure R2 illustrates the vertical cross section of GPH at these three different locations (Yellow stars). From this figure it is clear that vertical extent is difficult to obtain using fixed GPH.

We have also obtained composite mean spatial distribution of GPH and wind vectors at different pressure levels during different months to verify the vertical

structure of ASMA (Figure R3). The wind vectors also show anticyclone structure at 200 hPa and 150hPa. However, the spatial structure of GPH extends south at 150 hPa and 200 hPa conversely shifts towards north at 70 hPa and 50 hPa. Clear spatial structure of ASMA can be visible at 100 hPa only.

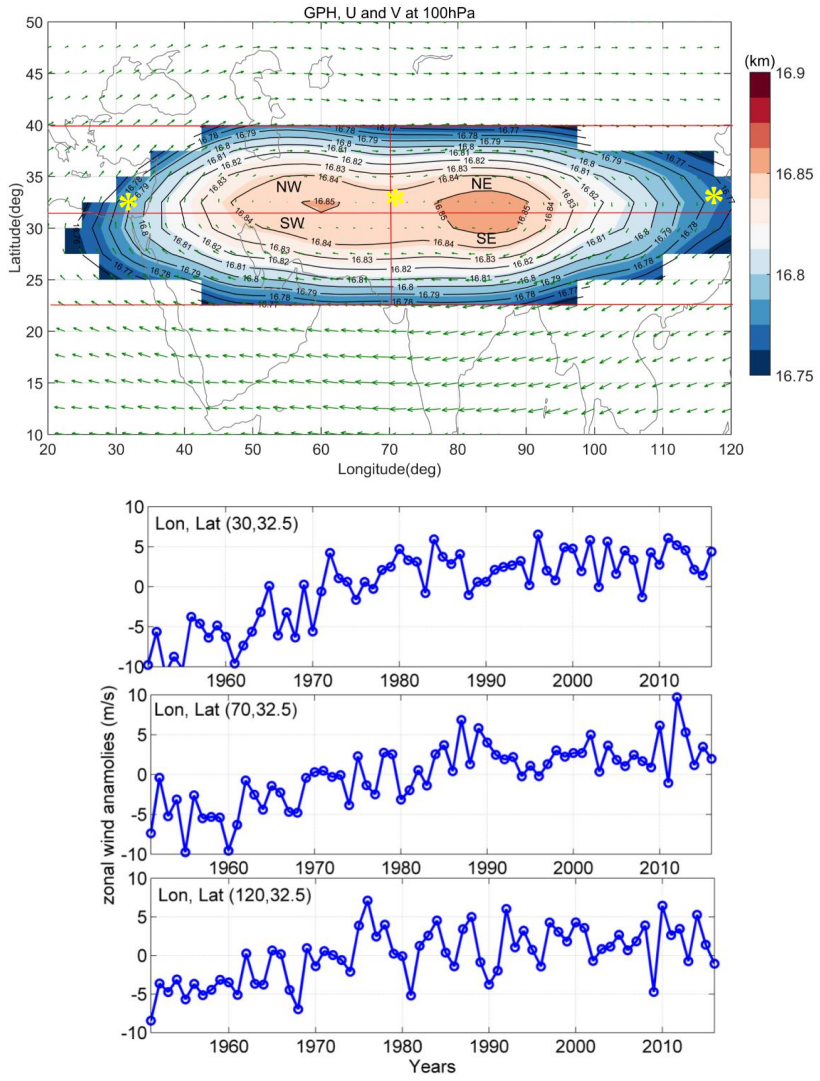

Figure R1. (Top) Climatology of GPH showing ASMA. (Bottom) Time series of zonal wind anomalies at different locations (mentioned with yellow stars) in ASMA region from NCEP reanalysis data during 1951-2016.

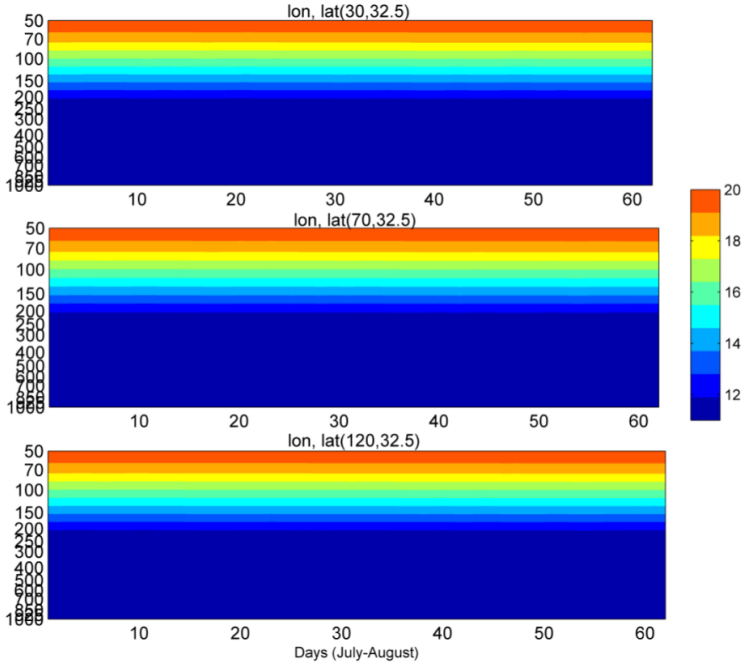

Figure R2. Vertical cross section of GPH at three different locations.

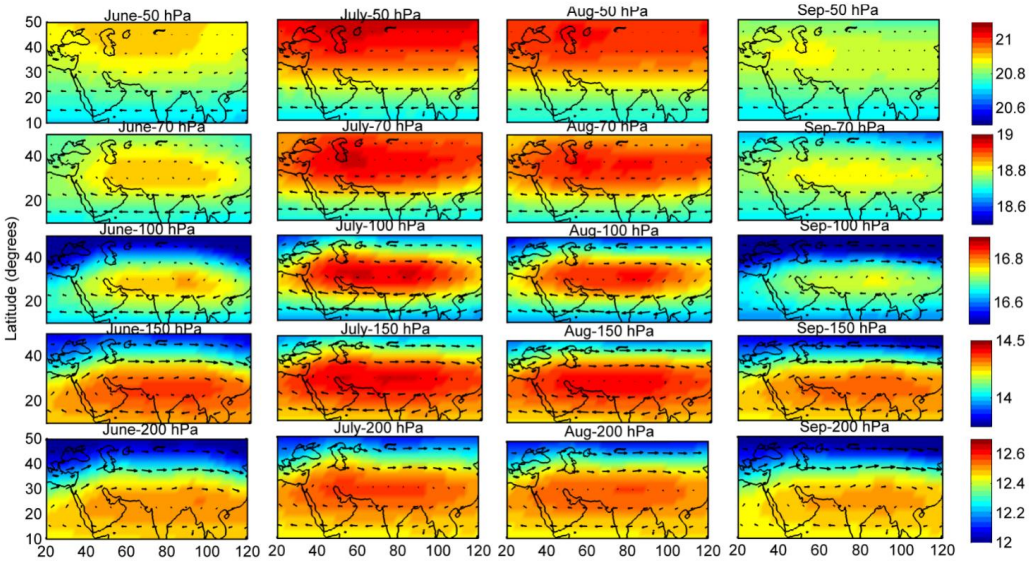

Figure R3. Composite mean spatial distribution of GPH and wind vectors at different pressure levels during different months.

(4) The study delineates that there is significant trend/difference in the ASMA during different decades during the period 1950-2016. The study period of ASMA variability shown in Figures 6, 7, and 8 are not clear (for active/break days, strong/weak monsoon years, and El Nino/La Nino years). Is it during the period 1948- 2016. The period of wind anomalies and temperature anomalies are not clear from the figure caption (from CHAMP and COSMIC). I think it is better to compare the variabilities for the same period. The ASMA variability for

the same period as that of the COSMIC and CHAMP data can be looked into. If already, it is done so, fine. However, this is not clear from the description of the figure caption and in the text.

Reply: In the revised version of the manuscript, we have considered the NCEP reanalysis (wind and temperature) data from 1951 onwards only for Figure 6, 7, 8. Only the tropopause which is shown in Figure 6, 7 and 8 are derived from GPSRO (CHAMP and COSMIC) satellite data which is available from the year 2002 onward only. Compared to previous and other existing data sets, this has the highest resolution and accuary in the UTLS region at present. Note that major features will not change by choosing different time period in this aspect.

(5) I understand that this manuscript is a part of a special issue 'Interactions between aerosols and the South West Asian monsoon'. However, this aspect is not much discussed in the manuscript. It would be nice if the authors can focus more on it.

Reply: In the revised manuscript we have mentioned it clearly in the introduction and discussion section regarding importance of aerosols and trace gases variability in ASMA. Since the half part of the manuscript discusses the influence of Indian summer monsoon, we have submitted the manuscript to this special issue.
Further, we have discussed the variability in trace gases and aerosols in ASMA and their relation with tropopause parameters in a separate paper which is also in ACPD.' Basha, G., Ratnam, M. V., Kishore, P., Ravindrababu, S., and Velicogna, I.: Influence of Asian Summer Monsoon Anticyclone on the Trace gases and Aerosols over Indian region, Atmos. Chem. Phys. Discuss., https://doi.org/10.5194/acp-2019-743, in review. This aspect also we have included in the revised version.

Specific comments: Abstract: Page1 Line 9: 'These pollutants. . .'-restructure the sentence —

Reply: Modified.

–Line11-12: 'The pollutants are expected to make a large radiative forcing'— Name the pollutants (species) responsible for large magnitude of radiative forcing —

Reply: Surface pollutants such as (CO, CH3Cl). As per reviewer suggestion, the basic introduction lines are removed. The same was suggested by another reviewer.

-Line13: long term oscillations such as .....

Reply: Long term oscillations are QBO and ENSO.

—-Line 19-20: 'Significant.....of the ASMA'. Significant decadal variability is observed with reference to 1951-1960 period. Restructure the sentence. ——

Reply: The sentence is reframed as 'Significant decadal variability is observed in the northeast and southwest parts of ASMA with reference to the 1951-1960 period'.

Line 21: 'Drastic increase from westerly to easterly'- What does the sentence really mean? (later in Section 3 in Figure 5, it is seen that anomalies are obtained by removing the mean

and strength is obtained by taking the difference of winds at difference latitudinal sectors. In that case is it possible to call the change of sign in anomalies as westerlies or easterlies?)

Reply: Thank you for rising this point. In the revised version we have mentioned it as anomalies.

Introduction Page 2 line 39: "distant maxima characters" Is it a typo error. Did you mean "distinct maxima characteristics" ——

Reply: Yes. We have changed in the revised version as 'distinct maximum characteristics'

line 41: 'The maximum occurs due to strong winds? Rewrite this sentence. The wind in the core of the anticyclone are not strong. Distinct maxima in tracers discussed in next paragraph also. Hence, authors may combine the sentences in first and second paragraph of section 1.

Reply: We have deleted this sentence in the revised version to avoid confusion and combined both the paragraphs.

line 46: modify the word 'issue' find another suitable word ——

Reply: Replaced 'issue' with 'problem'

line 50: 'confined tracers transported outside—'- What does this sentence mean?

Reply: We have modified the sentence in the revised version as 'The tracers which are transported are confined in the anticyclone will affect the trace gas concentration in the UTLS resulting in significant changes in radiative forcings (Solomon et al., 2010; Riese et al., 2012; Hossaini et al., 2015)'

Page 3 line 53: delete 's' of Plateaus

Reply: Deleted.

Data and methodology
Page 3 line 71: delete 's' of Centres

Reply: Deleted.

Section 2.2: Line 89 & 93: Specify the real data period used. Whether it is 1901-2016 or 1948-2016?

Reply: The whole analysis was done from the 1951 to 2016. This was clearly mentioned in manuscript.

Results and discussions
Figure 3: caption is missing. What is the confidence level of the trend shown? Compared to the trends in the northern end, trend in the southern edge seems to be very feeble?

Reply: Figure caption was overlapped with figure 3. In the revised version of the manuscript, we made it visible. Trends were estimated by using robust regression analysis at 95% confidence interval. The trends at northern end are significant than southern end and this point was added in the manuscript.

Page 8 Line185: Is it the time series of area/spatial average of zonal wind anomalies? . . ..

Reply: Yes. The wording is changed in the revised version.

Line 192: 'contaminated. . .' ? ———

Reply: We have re-written this sentence with better clarity in the revised manuscript.

Line 193-194: 'One is located. . .....and the other in the .....

Reply: These sentences were removed in the revised version as it is creating confusion to the reader.

Rewrite the sentence Figure 5e: Why sector 30◦ -40◦ is used. This region doesn't really represent the anticyclone according to figure 4.

Reply: We have followed the same procedure as reported Yuan et al., (2019) for estimating the strength of the anticyclone as difference in zonal winds between northern (30 ^{o} –40^{o} N) and southern (10 ^{o} –20 ^{o}N) flanks of the ASMA.

Yuan, C., Lau, W. K. M., Li, Z., and Cribb, M.: Relationship between Asian monsoon strength and transport of surface aerosols to the Asian Tropopause Aerosol Layer (ATAL): interannual variability and decadal changes, Atmos. Chem. Phys., 19, 1901–1913, https://doi.org/10.5194/acp-19-1901-2019, 2019.

However as per reviewer suggestion, we have estimated the strength of the ASMA by taking difference in zonal wind between northern (22.5 ^{o}N-40^{o}N) and southern (10^{o}N-20^{o}N). The modified figure is added in the revised version. It should be noted that, significant difference is not observed.

Page 8, Figure 5: Throughout the trend analysis section, the 'shift towards westerlies'. Whether the wind is becoming westerly or becoming less easterly (ie, the strength of the easterly is reduced). Whether it is really describing the strength of the anticyclone.

Reply: We are sorry for this mistake. In the revised version, we have mentioned it has zonal wind anomalies instead of easterly or westerly. The strength of the anticyclone was described by Yuan et al (2019) and similar method have been followed in the present study.

In Figure 5, anomalies are obtained by removing the mean and strength is obtained by taking the difference of winds at difference sectors. In that case is it possible to call the change of sign in anomalies as westerlies or easterlies ?)

Reply: Thank you for raising this important point. In the revised version, we used zonal wind anomalies only.

Page 9 Line 204: remove the bracket before 'during'

Reply: Removed.

Page 9 Line 221-222: whether easterly wind corresponds to cooler regions? Correct the sentence

Reply: Easterly wind corresponds to warmer region. This is corrected in the revised version.

Page 10 Line 237: 'Further, ...'rewrite the sentence

Reply: This sentence is modified in the revised version as 'The composite of mean distribution of the anticyclone circulation during strong and weak monsoon years is shown in Figure 7a based on GPH values at 100 hPa from NCEP reanalysis data'

Page 10 Line 240: In figure 6 the blue doesn't seem to be weak. The red and blue, strength are same but opposite in direction

Reply: This sentence is changed in the revised version of the manuscript as 'The circulation expands on the eastern and western sides of the anticyclone during the strong monsoon years (red line)'

Page 10, Line 242: Check this sentence for the correctness of "right (left) side of the anticyclone

Reply: This is corrected in the revised version.

Page 12 Lines 278-281: Check the figures and conclude the features seen in the figure only

Reply: Thank you for your suggestion. We have edited in the revised version.

Once again, we would like to thank the reviewer for his/her thoughtful comments and suggestions that led to substantial improvements in the revised manuscript.

---END---

Replies to Reviewer #3 Comments/Suggestions

This is a quite interesting paper related to the Asian summer monsoon anticyclone (ASMA) and the title is adequate. The research topic is of scientific interest and worth to be publishable. The study deals with the temporal, spatial and long term trends in the ASMA by using reanalysis and satellite data sets. The authors investigated the decadal variation of the anticyclone region with respect to 1951-1960 base period. They noticed significant changes over the anticyclone edges. Furthermore, the authors also studied the ASMA variability with respect to the wet and dry spells of the Indian monsoon, strong and weak monsoon years, and the stronger El Nino Southern Oscillation (ENSO) years. Overall, the authors have brought out some significant shortcomings from the study. However, I personally think that the paper still needs significant changes before the manuscript is ready for publication. Therefore, I recommend for publication in ACP with revision. I had the chance to read the comments of the Anonymous Reviewer #2 and I do share all his/her general comments.

Reply: First of all we wish to thank the reviewer for handling this manuscript and for offering his/her constructive comments/suggestions, which improved the manuscript content significantly. In the revised version, we have taken care of the reviewers comments/suggestions and we hope the reviewer will find the revised version satisfactory. As per reviewer suggestion, the methodology part and structure of the manuscript is changed compared to previous version.

General comments

1. Abstract needs to be improved. I strongly suggest the authors have to rewrite the entire abstract part and strictly focused on the important results obtained from the study.

Reply: In the revised version of the manuscript, we have changed the abstract by focusing on main results only.

2. How authors define the ASMA region? Why GPH values are considered to define the ASMA region? Other methods are also (for example potential vorticity) used by the previous researchers. Authors can stress this point and define their selection of ASMA region from the GPH values in the manuscript.

Reply: We have mentioned clearly the reason for selecting the GPH values in this study in section 3.1 with complete details and references.

'The spatial extent of anticyclone circulation is clearly evident in the grid 15^{o}N-45^{o}N; 30^{o}E- 120^{o}E at 100 hPa level and the climatological averaged values of GPH varies from 16.5-17 km in NCEP reanalysis during 1948-2016. Using the modified potential vorticity equation, Randel et al. (2006) showed the spatial variation of anticyclone where GPH values are stationary in the range of 16.75-16.9 km. Similarly, Park et al. (2007) showed the anticyclone structure from the strongest wind at 100 hPa through streamline function. Bian et al. (2012) reported the spatial variability of anticyclone using 16.77 km and 16.90 km in the GPH contour as the lower and the upper boundary, respectively. Thus, these empirically selected GPH values represent anticyclone boundaries. Therefore, in this present study, we have chosen the values from 16.75 to 16.9 km to investigate the spatial features of the anticyclone'.

3. Why authors separated the ASMA into 4 parts? This needs to be discussed properly.

Reply: In the revised version, we have given following reason for dividing the ASMA into 4 different regions.

The spatial trend analysis of ASMA shows distinct variability throughout the region and the edges of the ASMA undergo drastic variability compared to other regions. Therefore, in order to understand the asymmetry in the anticyclone variability, we have divided the anticyclone region into 4 different sectors as shown in Figure 4 based on the peak values of GPH along longitude and latitude cross-sections.

4. Conclusions part looks much generalized. The authors can provide 3 or 4 major results as point by point at the end of the conclusion part.

Reply: During the first review when we submitted the manuscript, one of the reviewers suggested to remove point by point list of conclusions. Therefore, we have written the summary and conclusion part in a paragraph.

5. Finally, the presentation quality needs 'strong improvements'.

Reply: In the revised version of the manuscript, we have taken care of grammatical mistakes, general statements and other points raised by the both reviewers.

Specific comments: There are some numbers of language and grammar issues in the present manuscript. However, I do not mention all of them in the present review. The authors should take care of all in the revised version of the manuscript.

Reply: In the revised version of the manuscript, we have taken utmost care to reduce the typos and grammatical mistakes to the maximum possible extent.

Line 7-16: Authors can shift these sentences into the introduction section.

Reply: As per reviewer suggestion, we have sifted some of these lines to the introduction section.

Line 18-19: 'The decadal variability of the anticyclone is very large at the edges of anticyclone than at the core region' rewrite the sentence. . .

Reply: In the revised version of the manuscript, we have rewritten this sentence as 'Significant decadal variability is observed in the northeast and southwest parts of ASMA with reference to the 1951-1960 period'

Line 20: change into 'to the 1951-1960 period'

Reply: Changed.

Line 22: change 'anticyclone' to 'the anticyclone'

Reply: Changed.

Line 29: '. . .. . .and during strong La Nina years'. Remove 'during' from the sentence.

Reply: Removed.

Line 30: Unclear——-'while interpreting the pollutants/trace gases in the anticyclone' Do you mean changes or variability in the trace gases? Please clarify what is meant here.

Reply: Written clearly in the revised version of the manuscript as 'It is suggested to consider different phases of monsoon while interpreting the variability of pollutants/trace gases in the anticyclone'

Line 35: 'from Asia to the Middle East'—— change it as 'from the Asia to Middle East'.

Reply: Changed.

Line 35: Add ‘The’ in front of ASMA. . .

Reply: Added.

Line 89-93: data period ‘1901-2016/1948-2016’. . .. . .This needs to be clarified.

Reply: Changed the year as per reviewer suggestion. The whole work is done for the period 1951-2016.

Line 94-124: The vertical resolution of GNSS RO data was missed. What is the original resolution of the GNSS RO (CHAMP and COSMIC). Is it originally available at 100/200m or some interpolation is done?

Reply: We have interpolated the data to 200m resolution and added in text.

Line 100-101: I doubt about the vertical resolution of 0.5-15 km? Is it correct? Authors can look on it again.

Reply: Sorry for this mistake. We have changed this in the revised manuscript as ‘The temperature profiles from this technique are available with low horizontal (~200-300 km) and high vertical resolutions (10-35 km) with an accuracy of <0.5 K’

Line 112: ‘The CHAMP data was available from 19 May 2001 to. . .. . .’ not required, delete this sentence.

Reply: Deleted.

Line 128-130: rewrite the sentence with clarity.

Reply: Rewritten in the revised manuscript.

Line 132-134: not clear. . .. ‘The spatial extent and intensity of anticyclone are greater during July compared to the intensities present during other months’. Rewrite the sentence.

Reply: Rewritten in the revised manuscript.

Line 135: Authors can follow any one either ‘Asia to the Middle East’ or ‘Middle East to East Asia’ in the entire manuscript. . . ... Authors mentioned earlier in Line 35 as ‘Asia to the Middle East’.

Reply: Thank you for your suggestion. We have followed Asia to Middle East throughout the manuscript.

Line 146: Authors written sometimes as ‘anticyclone’ sometimes as ‘the anticyclone’ in the entire manuscript. This needs to be solved in the entire manuscript.

Reply: Changed to ‘the anticyclone’.

Line 147: rewrite ’During the September month ’

Reply: Rewritten in the revised manuscript.

Line 150: change ‘the core region of anticyclone’. . .. The core region of the anticyclone.

Reply: Changed.

Line 159-173: The authors presented observed changes in the ASMA region during different decades. This paragraph needs some more discussion on the possible reasons for the observed changes.

Reply: In the revised version of the manuscript, we have added more discussion as per reviewer suggestion.

Line 174-175: I couldn't find 'Figure 3' in the manuscript.
Reply: Figure 3 was merged with Figure 2 in the previous version. However, in the revised manuscript, we have added this.

Line 199-203/Line 263-266: each sentence needs a citation. . ..I suggest add some references to the sentences. . ..
Reply: References added.

Line 253: 'excited'? It means existed? Check it once.
Reply: It should be exited.

Line257: This clearly demonstrates that a 'large scale ascent develops over the Asian monsoon region'. Incomplete sentence.
Reply: Modified in the revised version as 'This process clearly demonstrates that a large scale ascent develops over the Asian monsoon region'

Line 258-259: Unclear. Rewrite the sentence again.
Reply: This sentence is edited in the revised version as 'The transport processes from the boundary layer to the tropopause occur on the east side of the anticyclone i.e. southern flank of Tibetan Plateau, northeast India and the head of the Bay of Bengal'

Line 273-274: 'the strongest El Niño (1958, 1966, 1973, 1983, 1988, 1992, 1998, and 2015) and La Niña (1974, 1976, 1989, 1999, 2000, 2008, and 2011) years'. How authors selected these years? The temperature anomalies shown in Figure 8 are from NCEP or GNSS RO? If GNSS RO, how many years considered for obtaining the temperature anomalies?
Reply: We have chosen the strong ENSO years from the website (https://ggweather.com/enso/oni.htm). The background temperatures anomalies are shown in the Figure are from NCEP reanalysis data from 1951-2016. We have used only tropopause height data from GPSRO in Figure6, 7, and 8.

Line 307: change as 'reanalysis, satellite and observational data'
Reply: Changed.

Line 308: rewrite the sentence
Reply: Rewritten in the revised manuscript.

Line 309-310: unclear. 'Spatial (magnitude) of the anticyclone structure'
Reply: The spatial extent and intensity of the anticyclone is large during July compared to June and August.

Line 352-353: incomplete sentence.
Figures: Figure 3 was missed from the present manuscript.
Reply: Actually it was merged with figure 2. In the revised version of manuscript, we have added Figure 3 separately.

Rewrite the title of the Figure 4. . . '1948-2017' to ''1948-2016'. . ..
Reply: In the revised version, we have written clearly.

Figure captions needs to be improved with more clarity

Reply: In the revised version, figure captions are written in more elaborate way.

Once again, we would like to thank the reviewer for his/her thoughtful comments and suggestions that led to substantial improvements in the revised manuscript.

---END---

Asian Summer Monsoon Anticyclone: Trends and Variability

Ghouse Basha[1], M. Venkat Ratnam[1] and Pangaluru Kishore[2]
[1]National Atmospheric Research Laboratory, Department of Space, Gadanki-517112, India.
[2] Department of Earth System Science, University of California, Irvine, CA, 92697, USA.
Correspondence to: Ghouse Basha (mdbasha@narl.gov.in)

Abstract

The Asian Summer Monsoon Anticyclone (ASMA) has been a topic of intensive research in recent times through its variability in dynamics, chemistry and radiation. This work explores the spatial variability and the trends of the ASMA using observational and reanalysis data sets. Our analysis indicates that the spatial extent and magnitude of ASMA is greater during July and August compared to June and September. The decadal variability of the anticyclone is very large at the edges of the anticyclone than at the core region. Significant decadal variability is observed in the northeast and southwest parts of ASMA with reference to the 1951-1960 period. The strength of the ASMA shows a drastic increase in zonal wind anomalies in terms of temporal variation. Further, our results show that the extent of the anticyclone is greater during the active phase of the monsoon, strong monsoon years, and La Niña events. Significant warming with strong westerlies is observed exactly over the Tibetan Plateau from the surface to tropopause during the active phase of the monsoon, strong monsoon years, and during La Niña events. Our results support the transport process over Tibetan Plateau and the Indian region during active, strong monsoon years and during strong La Niña years. It is suggested to consider different phases of monsoon while interpreting the variability of pollutants/trace gases in the anticyclone.

Keywords: Asian Monsoon, anticyclone, geopotential height, La Niño, El Niño, and rainfall.

Deleted: ¶

Formatted: Font: Not Bold, Comple
Script Font: Not Bold

Formatted: Font: Not Bold, Comple
Script Font: Not Bold

Formatted: Indent: First line: 0.5"

Moved down [3]: The Asian Summe
Monsoon (ASM) dynamics act as a
pathway for the transport of trace gases
and pollutants both vertically (through
convection) and horizontally (through lo
level jet and tropical easterly jet). These
pollutants will be trapped in the
anticyclone present during the same peri
in the upper troposphere and lower
stratosphere (UTLS). Since the anticyclo
extends from the Middle East to East As
trapped pollutants are expected to make
large radiative forcing to the backgroun
atmosphere. Thus, it is essential to
understand the anticyclone features in
detail and its relation to long-term
oscillations.

Deleted: time

Formatted: Font: Not Bold, Comple
Script Font: Not Bold

Deleted: chemistry

Deleted:

Deleted: ¶

Formatted: Font: Not Bold, Comple
Script Font: Not Bold

Deleted:

Deleted: T

Deleted: Asian Summer Monsoon
Anticyclone (

Deleted:)

Deleted: Emphasis is made to investig
the temporal, spatial, and long-term tren
of ASMA.

Formatted: Not Highlight

Formatted: Not Highlight

Deleted: Significant deviations in the
northeast and southwest parts of ASMA
are also observed in the decadal variabil
with reference to 1951-1960 period.

Deleted: from the easterlies to the
westerlies

Deleted: during

Deleted: Over the Tibetan Plateau, th
is strong elevated heating from the surfa
to the tropopause, which is observed wit
strong westerlies during active and stron
monsoon years.

Formatted: Not Highlight

1. Introduction

The Asian Summer Monsoon Anticyclone (ASMA) is a dominant circulation in the Northern Hemisphere (NH) summer in the Upper Troposphere and Lower Stratosphere (UTLS), which extends from Asia to the Middle East. ASMA is bordered by the subtropical westerly jet in the north and easterly jets to the south. The Asian Summer Monsoon (ASM) dynamics act as a pathway for the transport of trace gases and pollutants both vertically (through convection) and horizontally (through low-level jet and tropical easterly jet). The ASMA circulation responds to heating corresponding to the deep convection of the south Asian monsoon (Hoskins and Rodwell, 1995; Highwood and Hoskins, 1998). This strong anticyclone circulation isolates the air and is tied to the outflow of deep convection, which has distinct maximum characteristics in terms of dynamical and chemical variability (Randel and Park, 2006; Park et al., 2007). Recently, the anticyclone circulation in UTLS has been paid more attention by researchers in order to understand the dynamics, chemistry, and radiation of the region. This problem has been discussed by several authors (e.g., Park et al., 2007; Fadnavis et al., 2014; Glatthor et al., 2015; Vernier et al., 2015; Santee et al., 2017). Deep convection during monsoon can transport tropospheric tracers from the surface to the UTLS (Vogel et al., 2015; Tissier and Legras, 2016). The tracers which are transported are confined in the anticyclone will affect the trace gas concentration in the UTLS resulting in significant changes in radiative forcings (Solomon et al., 2010; Riese et al., 2012; Hossaini et al., 2015). The center of the anticyclone is located either over the Iranian Plateau or over the Tibetan Plateau where the distribution of pollutants and tracers vary significantly (Yan et al., 2011).

The spatial extent, strength, and the location of an anticyclone vary on several temporal scales caused by internal dynamical variability of the Asian monsoon (Zhang et al., 2002; Randel and Park, 2006; Garny and Randel, 2013; Vogel et al., 2015; Pan et al., 2016).

Deleted: 1.

Formatted: Font: Bold, Font color: Black, Complex Script Font: Bold

Formatted: List Paragraph, Indent: Left: 0", Numbered + Level: 1 + Numbering Style: 1, 2, 3, … + Start 1 + Alignment: Left + Aligned at: 0.25" + Indent at: 0.5"

Moved (insertion) [3]

Deleted: The Asian Summer Monsoon (ASM) dynamics act as a pathway for th transport of trace gases and pollutants bo vertically (through convection) and horizontally (through low-level jet and tropical easterly jet). These pollutants w be trapped in the anticyclone present during the same period in the upper troposphere and lower stratosphere (UTLS). Since the anticyclone extends from the Middle East to East Asia, trapp pollutants are expected to make a large radiative forcing to the background atmosphere. Thus, it is essential to understand the anticyclone features in detail and its relation to long-term oscillations.¶

Formatted: Font: Bold, Font color: Black, Complex Script Font: Bold

Deleted: ¶

Formatted: Font color: Black, Not Highlight

Formatted: Widow/Orphan control

Deleted: the

Deleted: ant

Deleted: a

Deleted: characters

Deleted: dynamical

Deleted: and chemical characteristics

Deleted: The maximum occurs due to strong winds and closed streamlines of a anticyclone, which isolate the air within the anticyclone and it is very dynamic in nature (e.g. Vogel et al., 2016). ¶

Deleted: issue

Deleted: tracers transported outside th edge of the anticyclone

Deleted: centre

Deleted: s

Formatted: Indent: First line: 0"

Deleted: ¶

However, the variability of the anticyclone structure and response to Indian monsoon activity are not understood. Further, the tracers (O3, and CO etc.,) trapped in the anticyclone during the same period in the UTLS region. Since the anticyclone extends from the Middle East to East Asia, trapped pollutants are expected to make a large radiative forcing to the background atmosphere. Thus, it is essential to understand the variability of anticyclone structure itself in detail and its response to Indian Summer Monsoon (ISM). Therefore, in the first part of the study, we investigate the spatial, inter-annual and decadal variations of the anticyclone. Since the Indian monsoon responds at different time scales, we also investigated the anticyclone variability with respect to the active and break spells of the Indian monsoon, strong and weak monsoon years, and the stronger El Nino Southern Oscillation (ENSO) years. For this, we have utilized the NCEP/NCAR reanalysis geopotential height from 1951 to 2016. The structure of the paper is as follows. We describe the data sets used in this study in Section 2. Section 3 contains the seasonal and decadal variation of the anticyclone. Section 4 shows the influence of ISM on anticyclone i.e. active and break spells, strong and weak monsoon years, and ENSO's effects on the anticyclone. Finally, we discuss our results presented in Section 5.

Deleted: s

Deleted: monsoon

Deleted: in

Deleted: wet

Deleted: dry

Deleted: 1948

Deleted: and its relation with large sc oscillations

Deleted: days with wet

Deleted: dry

2. Data and Methodology

2.1. NCEP/NCAR Reanalysis

The National Center for Environmental Prediction (NCEP), in collaboration with the National Center for Atmospheric Research (NCAR) produces reanalysis data from a consistent assimilation and modeling procedure that incorporates all the available observed conditions obtained from conventional and satellite information from 1951 to the present (Kalnay et al. 1996). We used NCEP/NCAR reanalysis daily geopotential height (GPH) and wind data from the years 1951 to 2016. The NCEP/NCAR data assimilation uses a 3D-variational analysis scheme with 28 pressure levels and triangular truncation of 62 waves (horizontal resolution of 200m). Both GPH and temperature at the chosen standard levels are

Deleted: s

Deleted: 1948

Deleted: 1948

described as class output variables (Kalnay et al. 1996) i.e. they are strongly influenced by observed data. Only the Indian summer monsoon months (June, July, and August, September) containing gridded daily data were considered in this study. The NCEP/NCAR reanalysis data had a spatial resolution of 2.5°. The seasonal values are estimated from daily data. To identify the spatial and temporal variations of the anticyclone center, we used the monthly mean values of the GPH and the zonal wind component. The quality of NCEP GPH reanalysis data can be found from Bromwich et al. (2007).

2.2. IMD Gridded Precipitation Data

The India Meteorological Department (IMD) high-resolution (0.25°x0.25°) gridded precipitation data is used to identify the active and break spells during June, July and August months from 1951-2016. This precipitation data has been validated extensively with observational and reanalysis data sets and displays a very good correlation (Kishore et al., 2016). For identification of active (or wet) and break (or dry) spells, we followed a similar procedure as described by Rajeevan et al. (2010) and Pai et al. (2016) over the monsoon core zone (18°N-28°N, and 65°E-88°E). Data from 1951-2016 have been used.

2.3. GNSS Radio Occultation (RO) Data

We have also used the Global Navigation Satellite System (GNSS) Radio Occultation (RO) data for investigating the temperature anomaly. The basic measurement principle of RO exploits the atmosphere-induced phase delay in the GNSS signals, which are recorded in the low earth-orbiting satellite. This technique provides vertical profiles of refractivity, density, pressure, temperature, and water vapor (Kursinski et al., 1997). The temperature profiles from this technique are available with low horizontal (~200-300 km) and high vertical resolutions (10-35 km) with an accuracy of <0.5 K. We used the CHAllenging Minisatellite Payload (CHAMP) and Constellation Observing System for Meteorology, Ionosphere, and Climate (COSMIC) covering the period from 2002 to 2016.

Deleted: s

Deleted: ,

Deleted: wet

Deleted: dry

Deleted: 1901

Deleted: the

Deleted: 1948

Deleted:

Deleted: vapour

Deleted: 0.5

Deleted: 15

The CHAMP satellite was launched on 15 July 2000 into a circular orbit by Germany to measure the Earth's gravity and magnetic field and to provide global RO soundings (Wickert et al. 2001). About ~230 RO profiles per day were measured by the CHAMP payload since 2002. The CHAMP payload was solely designed to track the setting occultations, and the RO event gets terminated when the signal is lost, which results in a decrease in the number of occultations with a decreasing altitude (Beyerle et al. 2006). This receiver measures the phase delay of radio wave signals that are occulted by the Earth's atmosphere. From this phase delay, it is possible to retrieve the bending angle and refractivity vertical profiles.

COSMIC consists of a constellation of 6 satellites, which was launched in April 2006 to a circular, 72° inclination orbit at a 512 km altitude capable of receiving signals from the Global Positioning System (GPS) (Anthes et al., 2008). Compared to previous satellites, COSMIC satellites employed an open loop mode, which can track both the rising and setting of occultations (Schreiner et al. 2007). The open-loop tracking technique significantly reduces the GPS RO inversion biases by eliminating tracking errors (Sokolovskiy et al. 2006). The COSMIC temperature profiles display a very good agreement with radiosonde data, reanalyses, and models (Rao et al., 2009; Kishore et al., 2011; Kishore et al., 2016). The CHAMP and COSMIC GPSRO data was interpolated to 200 m from their native resolution. We derived the cold point tropopause altitude/temperature over the ASMA region as discussed by Ratnam et al. (2014) and Ravindrababu et al. (2015). Both the CHAMP and COSMIC data were obtained from COSMIC Data Analysis and Archive Center (CDAAC) (https://cdaac-www.cosmic.ucar.edu/cdaac/products.html).

3. Results and Discussion

3.1. Variability of the Anticyclone

Deleted: in to

Deleted: The CHAMP data was available from 19 May 2001 to 5 Octobe 2009.

Deleted: ¶

The climatological spatial variability of the GPH and wind vectors at 100 hPa during June, July, August and September months from NCEP reanalysis data is shown in Figure 1(a, b, c & d). The anticyclone circulation is clearly depicted during June, July, August, and September by wind vectors (Figure 1). During the month of September and June, the values of GPH are low compared to July and August which represents the spatial extent of the anticyclone. The spatial extent and intensity of the anticyclone are greater during July compared to the other months. During July and August, the anticyclone extends from East Asia to the Middle East. The spatial extent of the anticyclone circulation is clearly evident in the grid 15^{o}N-45^{o}N; 30^{o}E-120^{o}E at 100 hPa level and the climatological averaged values of GPH varies from 16.5-17 km in NCEP reanalysis during 1951-2016. Using the modified potential vorticity equation, Randel et al. (2006) showed the spatial variation of the anticyclone where GPH values are stationary in the range of 16.75-16.9 km. Similarly, Park et al. (2007) showed the anticyclone structure from the strongest wind at 100 hPa through streamline function. Bian et al. (2012) reported the spatial variability of the anticyclone using 16.77 km and 16.90 km in the GPH contour as the lower and the upper boundary, respectively. Thus, these empirically selected GPH values represent the anticyclone boundaries. Therefore, in this present study, we have chosen the values from 16.75 to 16.9 km to investigate the spatial features of the anticyclone and the resultant picture is depicted in Figure 1(e, f, g & h). The spatial extent and existence of the anticyclone are highly prominent during July and August compared to June. During the September month, very low values of GPH are seen compared to July and August. Therefore, we considered the average of July and August GPH from 1951-2016 for further analysis as shown in Figure S1. The core region and the spatial extent of the anticyclone are clearly evident from Figure S1. The core region of the anticyclone shows bimodal distribution i.e. one core located at the south-western flank of the Himalayas and another over Iran. The core region over the south-western flank of

Deleted: C
Deleted: along
Formatted: Indent: First line: 0.5"
Deleted: August
Deleted: June
Deleted: of
Deleted:
Deleted: intensities present during
Deleted: the
Deleted: to East Asia
Deleted: 1948
Deleted: is
Deleted: the
Deleted: values in the range 16.75-16. km are not present
Deleted: .
Deleted: 1948

Himalayas is due to large scale updraft, which is caused by the moist energy over Indo-Gangetic plain, heating of Tibetan plateau, and the orographic forcing of the Himalayas. Severe heating over Arabian Peninsula supports the formation of the mid-tropospheric the anticyclone in the west. This anticyclone can merge intermittently within ASMA. It is also observed that the spatial extent of the anticyclone varies drastically at different temporal scales. Therefore, seasonal variation is much more pronounced.

The decadal variation of the anticyclone is studied with respect to the spatial variability. Figure 2 shows the decadal spatial variation of the anticyclone with reference to the years 1951-1960. The significant difference in the decadal variation is noticed in Figure 2. The edges (east, north, and west) of the anticyclone undergo drastic changes during the period 1961-1970. In case of 1971-1980 period, except for a small portion in the east, the whole anticyclone shows drastic changes. During the decade 1971-1980, the recorded GPH values in the anticyclone are lower by ~ 25 m when compared to the values in 1951-1960. This feature is quite opposite during 1981-1990 where high values (~30 m) are observed compared to those in the reference period. The GPH difference is significant over the west, northeast and southern regions of the anticyclone during the 1991-2000 period. Similar changes are observed during 2001-2010. Compared to all the decadal differences, 2011-2016 shows a completely different picture. The changes are only in the western and north-eastern corner, whereas other parts of the anticyclone do not show any change. From this analysis, we observed significant changes in the anticyclone even from one decade to another, which can result in a change in chemical and dynamical changes over this region.

Further, the spatial distribution of trend is estimated during the years 1951-2016 by using robust regression analysis at 95% confidence interval as displayed in Figure 3. The edges on all sides of the anticyclone undergo noticeable changes compared to the core region. The east and north-west side of the anticyclone shows an increasing trend compared to other

Formatted: Indent: First line: 0", Widow/Orphan control

Deleted: from

Deleted: ¶

Formatted: Widow/Orphan control

Deleted: s

Deleted: 1948

Deleted: Spatially, the anticyclone tre shows two distinct pictures

Moved (insertion) [4]

Deleted: and is

regions. The trends at the northern end are significant than the southern end. A few portions on the northern side of the anticyclone show a reduction in the strength. Therefore, in order to understand the asymmetry in the anticyclone variability, we have divided the anticyclone region into 4 different sectors as shown in Figure 4 based on the peak values of GPH along longitude and latitude cross-sections. The center values of GPH are located at 70°E longitude and 32.5°N Latitude. The four sectors can be divided into South-East (SE) (22.5°N-32.5°N), North-East (NE) (32.5°N-40°N) in the longitude band of 70°E-120°E, South-West (SW) (22.5°N-32.5°N), and North-West (NW) (32.5°N-40°N) at the 20°E-70°E longitude range. The area-averaged time series (July and August) of zonal wind anomalies in these sectors from 1951-2016 are shown in Figure 5. The zonal wind anomalies show a clearly increasing trend in all the sectors. From the year 1951 to 1980, the zonal wind anomalies are negative and shift to positive in all the sectors. The year 1980 represents the beginning of industrialization globally (Basha et al., 2017). The change is highly significant in the north-west and north-east sectors with a magnitude variability of 7.59 m/s from 1951-2016 whereas it is 5.44 m/s in the south-east and south-west sectors. In addition, we estimated the strength of the anticyclone during the monsoon season by using a difference in the zonal wind between the northern (30°N-40°N) and southern (10°N-20°N) flanks of the anticyclone, which is depicted in Figure 5e. A significant increase in the strength of the anticyclone is noticed from Figure 5e at a rate of 0.157 m/s per year (10.36 m/s from 1951-2016).

It is well known that the Indian monsoon rainfall varies at different time scales i.e. daily, sub-seasonal, interannual, decadal and centennial scales (Rajeevan et al., 2010). Precipitation during the monsoon varies from intra-seasonal scales between active (good rainfall) and break (less rainfall) spells. Any small change in the precipitation pattern will affect the anticyclone due to the thermodynamics involved in rainfall. In this study, we also investigated the anticyclone variability during the active and break spells of the Indian

Moved up [4]: The edges on all sides the anticyclone undergo noticeable changes compared to the core region.
Deleted: The
Deleted: shows
Deleted: (~30 m)
Deleted: whereas the southern part illustrates increases in strength
Deleted: As noticed from Figure 3, the spatial trend analysis of ASMA shows distinct variability throughout the regio
Deleted: as
Deleted:
Deleted: 1948
Formatted: Complex Script Font:
Deleted: shows
Formatted
Deleted: 1948
Formatted: Complex Script Font:
Formatted
Formatted: Complex Script Font:
Formatted
Deleted: are
Formatted: Complex Script Font:
Formatted
Deleted: easterlies and later on, a cle
Formatted: Complex Script Font:
Formatted
Formatted
Formatted
Formatted
Deleted: .
Formatted: Complex Script Font:
Formatted: Font: Bold
Formatted
Deleted: This represents that the
Formatted: Font: Bold
Deleted: 10
Deleted: 1948
Deleted: It is to be noted that the win
Formatted: Highlight
Deleted: 184
Deleted: 12
Deleted: 1948
Deleted: 2018
Deleted: ¶
Deleted: little
Deleted: (

monsoon. The active and break spells were identified in July and August by using the high resolution gridded (0.25^o x 0.25^o) rainfall data from 1951 to 2016 as defined by Pai et al. (2010).

The number of active and break days is derived from the precipitation data shown in Figure S2 (a & b). Daily GPH, temperature, and zonal wind are taken from NCEP reanalysis whereas the tropopause altitude is derived from the GNSS RO data for active and break days. The anticyclone structure during active (red line) and break (blue line) days are shown in Figure 6a. Two interesting aspects of the anticyclone variability can be noticed between active and break days. One aspect is the extent of the anticyclone is large during active days compared to break days and another is the existence of two cell structures in the anticyclone core region during active days. The extent is large in the eastern and northern side in active days. The zonal (meridional) cross-section of temperature (color shade), zonal wind (contour lines) difference between active and break phase averaged in the longitude band of 80^oE-90^oE (latitude band of 30^oN-40^oN) along with cold point tropopause for active and break days is illustrated in Figures 6b & 6c. During active days, temperature shows cooling in tropical latitudes whereas it shows warming in the mid-latitudes from surface to the tropopause. Significant warming is observed during the active days in the mid-troposphere over the Tibetan Plateau and its northern side. Westerly (easterly) winds exist over the cooler (warmer) regions. The warm temperature anomalies stretch from 1.5 to 12 km in between 25^oN and 60^oN. The tropopause altitude is low (high) during the active (break) phase of Indian monsoon as shown in Figure 6b. The meridional cross-section of temperature anomalies displays significant warming from ~1.5 to 8 km over the Indian region. The tropopause altitude exemplifies random variability in the meridional cross-section.

As discussed previously, the anticyclone circulation is significant during the months of July and August when most of the precipitation occurs over India (Basha et al., 2013;

Deleted: 1948

Deleted: extent of

Deleted: in active

Deleted:

Deleted: the

Deleted: and cooler

Deleted:

Basha et al., 2015; Kishore et al., 2015; Narendra Reddy et al., 2018). The influence of strong and weak monsoon years will have a drastic impact on anticyclone circulation. In order to understand these changes, we have divided the years into strong and weak monsoon years based on gridded precipitation data over the domain 5°N-30°N and 70°E-95°E from the years 1951-2016. This region is known to have heavy precipitation and orographic forcing, which helps transport of water vapor through deep convection to UTLS (Houze et al., 2007; Medina et al., 2010; Pan et al., 2016). The detrended precipitation represents the strong and weak monsoon years. Years with positive (negative) values of precipitation shows the strong (weak) monsoon years as shown in Figure S2b.The composite of mean distribution of the anticyclone circulation during strong and weak monsoon years is shown in Figure 7a based on GPH values at 100 hPa from NCEP reanalysis data. The circulation expands on the eastern and western sides of the anticyclone during the strong monsoon years (red line). The core of the anticyclone is significant during strong monsoon years. Clear eye structure is observed in the core of the anticyclone on left (right) during the strong (weak) monsoon years. The composite mean difference of temperature and zonal wind between the strong and weak monsoon years along with tropopause altitude averaged in the longitude range of 80-85°E is shown in Figure 7b. The warmest temperature anomalies are observed over the Tibetan Plateau. Positive (warm) temperature anomalies exactly above the Tibetan Plateau (11 km) and negative (cooling) on both sides are noticed in the lower troposphere from Figure 7b. Strong easterlies (westerlies) winds are observed on the left (right) side of the Tibetan Plateau. The whole Tibetan Plateau acts as a barrier that drives the cold air to upper altitudes during strong monsoon years. Strong anticyclone circulation with strong westerlies at 35°N and easterlies on both sides with elevated tropopause represent the impacts of the strong monsoon vertically above the anticyclone. The rising motion over East Asia is excited by the local heating of the Tibetan Plateau links to the single stretch vertically. The longitude and

Deleted: 1948

Deleted: vapour

Deleted: Further, we have divided the GPH, temperature at 100 hPa tropopause altitude based on strong and weak monsoon years.

Deleted: weak monsoon (blue line) ye

Deleted: on the right (left) side of the

Deleted: in the core region

Deleted: raising

altitude cross-section of temperature and wind anomalies shown in Figure 7c are averaged between a latitude band of 35-40^{o}N. Positive temperature anomalies are observed from the surface to 12 km in the longitudes 60-80^{o}E and stretch towards the west. This process clearly demonstrates that a large scale ascent develops over the Asian monsoon region. The tropopause altitude is high (low) during strong vertical motion and heavy precipitation is noticed over the region similar to that reported by Lau et al. (2018). The transport processes from the boundary layer to the tropopause occur on the east side of the anticyclone i.e. southern flank of Tibetan Plateau, northeast India and the head of the Bay of Bengal. This result is consistent with the previous studies by Bergman et al. (2013).

ENSO typically shows the strongest signal in boreal winter, but it can affect the atmospheric circulation and constituent distributions until the next autumn (McPhaden et al., 2006). It is well-known that strong ENSO events have a significant influence on tropical upwelling and STE. This change can impact the distribution of the composition and structure of the UTLS region. In the UTLS region, the tropopause responds to the annual and interannual variability associated with ENSO (Trenberth, 1990) and QBO (Baldwin et al., 2001). Several studies have been focused on the effects of the different impacts of El Niño on tropopause and lower stratosphere (Hu and Pan, 2009; Zubiaurre and Calvo, 2012; Xie et al., 2012). In the present study, we have investigated the changes associated with strong ENSO events with the anticyclone circulation and tropical upwelling during July and August. Therefore, we have also separated the GPH for the strongest El Niño (1958, 1966, 1973, 1983, 1988, 1992, 1998, and 2015) and La Niña (1974, 1976, 1989, 1999, 2000, 2008, and 2011) years to verify the change in the circulation pattern of the anticyclone. For this, we have chosen July and August GPH data at 100hPa as shown in Figure 8. The red and blue colors indicate the composite of the La Niña and El Niño circulation. During the La Niño, the anticyclone circulation is stronger and extends over the El Niña at 100 hPa as shown in the

Deleted: found

Deleted: occurs

Deleted: ¶

Deleted:

Deleted: this

Deleted: El

Formatted: Not Highlight

Deleted: La

Formatted: Not Highlight

Figure 8a. On the eastern and southern sides of the anticyclone, the expansion is more during the La Niña years. The warm temperature with strong westerlies in the latitude band of 43°N-55°N is observed during La Niño as shown in Figure 8b (Lau et al., 2018). The cooling impact is significant over the Tibetan Plateau during La Niña events compared to El Niño events. Significant cooling is observed over the Tibetan Plateau and distributes towards tropical latitudes between 600-100 hPa. The zonal wind shows a convergence of easterly winds over the Tibetan Plateau from the mid to the upper tropospheric region. On the right side of the Tibetan Plateau there exist strong westerly winds from the surface to the tropopause altitudes with strong warming. The meridional cross-section of temperature and the zonal wind difference between La Niña and El Niño is shown in Figure 8c. Significant cooling is observed during La Niña in the longitude band of 80°E-100°E with strong easterlies from the surface to the tropopause. From this analysis, it is clear that the Indian summer monsoon variability has a significant impact on ASMA, and it is necessary to consider the different phases of monsoon while dealing with UTLS pollutants. In addition, we have investigated the zonal mean vertical cross-section in the longitude band of 50-60°E, which represents the Iranian Mode. Figure S3 depicts the difference between active and break phases, strong and weak monsoon years, and La Niño and El Niño years along with the tropopause altitude. Significant warming is observed during La Niña years and strong monsoon years compared to the active phase of the Indian monsoon in the troposphere. Compared to the Tibetan mode, Iranian mode warming is less. The tropopause altitude is slightly higher during the active phase of the Indian monsoon, strong monsoon years and La Niña years. A moderate increase in tropopause from the equator to 40°N is observed and decreases drastically afterward.

Deleted: the
Deleted: El
Formatted: Not Highlight
Deleted: In
Deleted: the
Deleted: s

4. Summary and Conclusions

Several authors discussed the interannual and decadal variability of pollutants and tracers

in the ASMA region from the model, observational and reanalysis data sets (Kunze et al., 2016; Santee et al., 2017; Yuan et al., 2019). In this present study, we have investigated the spatial variability, trends of the anticyclone and the influence of Indian monsoon activity i.e. active and break days, strong and weak monsoon years, and strong La Niña and El Niño years on ASMA using long-term reanalysis, satellite and observational data sets that were not investigated earlier. In this study, we have considered the GPH values from 16.75 km to 16.9 km, which represents the spatial structure of the anticyclone at 100 hPa. Our analysis shows that the spatial extent (magnitude) of the anticyclone structure is very large (strong) during July followed by August whereas it is very weak in June at 100 hPa. The bimodal distribution (Tibetan and Iranian modes) of the anticyclone is clearly observed during the month of July which is absent during other months (June and August). The anticyclone variability undergoes significant decadal variations from one decade to another. The edges of ASMA changes drastically compared to the core of the anticyclone. However, there are significant spatial differences in the structure of the anticyclone at 100 hPa. The anticyclone undergoes a decreasing trend on the northern side whereas an increasing trend on the western part. A significant increasing trend is observed in the spatially averaged zonal wind in four different sectors (Figure 5). The zonal wind anomalies show increasing trend in all the sectors at 100 hPa. The change is significant in the north-western and north-eastern sectors with a magnitude variability of 7.59 m/s from 1951-2016 whereas it is 5.44 m/s in the south-eastern and south-western sectors. The strength of the anticyclone increases with a rate of 0.157 m/s per year (10.36 m/s from 1951-2016) in the anticyclone region (Figure 5e). Yuan et al. (2019) also reported the increasing trend in the strength of the anticyclone by considering the MERRA 2 reanalysis data from 2001-2015.

Further, we have investigated the Indian monsoon influence on the anticyclone region. Our results reveal that the spatial extent of the anticyclone expands during the active phase of

Deleted: and

Deleted:

Deleted: .

Deleted: W

Deleted: in this study

Deleted: , the

Deleted: not present

Deleted: anomalies

Deleted: illustrate easterlies from 1948 1951 to 1980 and westerlies thereafter. I the recent decade the westerlies are significant in the anticyclone region at 1 hPa.

Deleted: 10

Deleted: 48-

Deleted: 184

Deleted: 12

Deleted: 1948

the Indian monsoon, the strong monsoon years and during strong La Niña years on the northern and eastern sides. A similar expansion of the anticyclone is noticed during strong monsoon years from MERRA2 data by Yuan et al. (2019). However, the ASMA boundaries are not always well defined in all the events. The zonal mean cross-section of temperature shows significant warming over the Tibetan Plateau and from the surface to 12 km during the active phase of the Indian monsoon, the strong monsoon years, and the strong La Niña years. Similarly, the rise of tropopause during the active phase of the Indian monsoon, the strong monsoon years and the strong La Niña years are noticed. Since the Tibetan Plateau acts as a strong heat source in summer with the strongest heating layer lying in the lower layers, the thermal adaptation results in a shallow and weak cyclonic circulation near the surface, and a deep and strong anti-cyclonic circulation above it. During summer, the Tibetan Plateau acts as a strong heat source, which influences the whole UTLS region. The warm ascending air above will pull the air from below; the surrounding air in the lower troposphere converges towards the Tibetan Plateau area and climbs up the heating sloping surfaces (Bergman et al., 2013; Garny and Randel, 2016). Significant warming is observed over the Tibetan Plateau, which represents the strong transport of pollutants into the tropopause during the active phase of the Indian monsoon, the strong monsoon years, and the strong La Niña years. Pan et al. (2016) reported the transport of carbon monoxide through the southern flank of the Tibetan Plateau from the model analysis. The above-mentioned results indicate that the high mountain regions play a significant role in elevated heat sources during the formation and maintenance of the anticyclones over Asia. It emphasizes the role of the thermal forcing of the Tibetan Plateau on the temporal and the spatial evolution of the South Asian High. Lau et al. (2018) showed that the transport of the dust and pollutants from the Himalayas-Gangetic Plain and the Sichuan Basin.

Deleted: During these events, the bimodal distribution (Tibetan and Iranian modes) of the anticyclone is noticed.

Deleted: is

Deleted: m

Overall, we demonstrate the ASMA variability during different phases of the Indian monsoon. The uplifting of boundary layer pollutants to the tropopause level occurs primarily on the eastern side of the anticyclone, centered near the southern flank of the Tibetan Plateau, north-eastern India, Nepal, and north of the Bay of Bengal. The variability of tropopause altitude and temperature, trace gases (Water Vapour (WV), Ozone (O_3), Carbon Monoxide (CO) and aerosols (Attenuated Scattering Ratio (ASR) shows distinct in picture in ASMA region. The ASMA itself is highly dynamical in nature and the confinement of tracers and aerosols results in changes in its chemistry and radiation (Basha et al., 2019) However, a more detailed and higher quality of the dataset is needed to further understand the effects of the Tibetan Plateau on the transport of different tracers and pollutants to the UTLS region (Ravindrababu et al., 2019).

Deleted: a

Deleted: ¶

*Data Availability***.** The NCEP/NCAR reanalysis data are available from NOAA website (https://www.esrl.noaa.gov/psd/data/gridded/data.ncep.reanalysis.pressure.html). The COSMIC and CHAMP data is available from COSMIC CDAAC website. IMD gridded precipitation data is available at National Climate data center Pune, India. All the data used in the present study is available freely from the respective websites.

Authors'Contributions. GB and MVR conceived and designed the scientific questions investigated in the study. GB performed the analysis and wrote the draft in close association with MVR. PK estimated the active and break spells of the Indian monsoon. All authors edited the paper.

Deleted: cooperation

Competing Interests. The authors declare that they have no competing financial interests.

Acknowledgements. We thank NCEP/NCAR reanalysis for providing reanalysis data. We thank CDAAC for production of COSMIC and CHAMP GPSRO data and IMD gridded precipitation data from National Climate data center Pune, India. This work was supported by National Atmospheric Research Laboratory, Department of Space, and India

References

Anthes, R. A., Bernhardt, P. A., Chen, Y., Cucurull, L., Dymond,K. F., Ector, D., Healy, S. B., Ho, S.-H., Hunt, D. C., Kuo, Y.-H., Liu, H., Manning, K., McCormick, C., Meehan, T. K., Randel,W. J., Rocken, C., Schreiner,W. S., Sokolovskiy, S. V., Syndergaard, S., Thompson, D. C., Trenberth, K. E., Wee, T.-K., Yen, N. L., and Zeng, Z.: The COSMIC/Formosat/3 mission: Early results, B. Am. Meteorol. Soc., 89, 313–333, 2008.

Rao, D. N., Ratnam, M. V., Mehta, S., Nath, D., Ghouse Basha, S., Jagannadha Rao, V. V. M., Krishna Murthy, B. V., Tsuda, T., and Nakamura, K.: Validation of the COSMIC radio occultation data over Gadanki (13.48 N, 79.2 E): A tropical region, Terr. Atmos. Ocean. Sci., 20, 59–70, doi:10.3319/TAO.2008.01.23.01(F3C), 2009.

Baldwin, M. P., Gray, L. J., Dunkerton, T. J., Hamilton, K., Haynes, P. H., Randel, W. J., Holton, J. R., Alexander, M. J., Hirota, I., Horinouchi, T., Jones, D. B. A., Kinnersley, J. S., Marquardt, C., Sato, K., and Takahashi, M.: The quasi-biennial oscillation, Rev. Geophys., 39, 179–229, doi:10.1029/1999RG000073, 2001.

Basha, G., Kishore, P., Ratnam, M.V., Ouarda, T.B.M.J., Velicogna, I., and Tyler sutterly.: Vertical and latitudinal variation of the intertropical convergence zone derived using GPS radio occultation measurements, *Remote Sensing of Environment*, http://dx.doi.org/10.1016/j.rse.2015.03.024, 2015.

Basha, G. and Ratnam, M. V.: Moisture variability over Indian monsoon regions observed using high resolution radiosonde measurements, Atmos. Res., 132–133, 35–45, https://doi.org/10.1016/j.atmosres.2013.04.004, 2013.

Basha, G., Kishore, P., Ratnam, M. V., Jayaraman, A., Kouchak, A. A., and Taha, B.J. M.: Historical and projected surface temperature over India during the 20th and 21st century. *Scientific Reports*, 7(1), 2987. https://doi.org/10.1038/s41598-017-02130-3, 2017.

Deleted: http://dx.doi.org/10.1016/j.r 2015.03.024

Formatted: Font color: Text 1

Formatted: Font: Italic, Font color: Text 1, Complex Script Font: Italic

Formatted: Font color: Text 1

Basha, G., Ratnam, M. V., Kishore, P., Ravindrababu, S., and Velicogna, I.: Influence of Asian Summer Monsoon Anticyclone on the Trace gases and Aerosols over Indian region, Atmos. Chem. Phys. Discuss., https://doi.org/10.5194/acp-2019-743, in review, 2019.

Bergman, J. W., Fierli, F., Jensen, E. J., Honomichl, S., and Pan, L. L.: Boundary layer sources for the Asian anticyclone: Regional contributions to a vertical conduit, J. Geophys. Res., 118, 2560–2575, https://doi.org/10.1002/jgrd.50142, 2013.

Beyerle, G., Schmidt, T., Wickert, J., Heise, S., Rotacher, M., Koenig-Langlo, G., and Lauritsen, K. B.: Observations and simulations of receiver-induced refractivity biases in GPS radio occultation, J. Geophys. Res., 111, D12101, doi:10.1029/2005JD006673. 2006.

Bian, J., Pan, L. L., Paulik, L., Vömel, H., and Chen, H.: In situ water vapor and ozone measurements in Lhasa and Kunmin during the Asian summer monsoon, Geophys. Res. Lett., 39, L19808, doi:10.1029/2012GL052996, 2012.

Bromwich, D. H., Fogt, R. L., Hodges, K. I., and Walsh, J. E.: A tropospheric assessment of the ERA-40, NCEP, and JRA-25 global reanalyses in the polar regions, J. Geophys. Res.-Atmos., 112, D10111, doi:10.1029/2006JD007859, 2007.

Fadnavis, S., Schultz, M. G., Semeniuk, K., Mahajan, A. S., Pozzoli, L., Sonbawne, S., Ghude, S. D., Kiefer, M., and Eckert, E.: Trends in peroxyacetyl nitrate (PAN) in the upper troposphere and lower stratosphere over southern Asia during the summer monsoon season:regional impacts, Atmos. Chem. Phys., 14, 12 725–12 743, https://doi.org/10.5194/acp-14-12725-2014, 2014.

Garny, H. and Randel, W. J.: Dynamic variability of the Asian monsoon anticyclone observed in potential vorticity and correlations with 5 tracer distributions, J. Geophys. Res., 118, 13 421–13 433, https://doi.org/10.1002/2013JD020908, 2013.

Formatted: Font: Times New Roma 12 pt, Font color: Text 1, Complex Script Font: 12 pt

Formatted: Font color: Text 1

1231 Garny, H. and Randel, W. J.: Transport pathways from the Asian monsoon anticyclone to the
1232 stratosphere, Atmos. Chem. Phys., 16, 2703-2718, https://doi.org/10.5194/acp-16-2703-
1233 2016, 2016.
1234 Glatthor, N., Höpfner, M., Stiller, G. P., von Clarmann, T., Funke, B., Lossow, S., Eckert, E.,
1235 Grabowski, U., Kellmann, S., Linden, A., Walker, K. A., and Wiegele, A.: Seasonal and
1236 interannual variations in HCN amounts in the upper troposphere and lower stratosphere
1237 observed by MIPAS, Atmos. Chem. Phys., 15, 563–582, https://doi.org/10.5194/acp-15-
1238 563-2015, 2015.
1239 Gottschaldt, K.-D., Schlager, H., Baumann, R., Cai, D. S., Eyring, V., Graf, P., Grewe, V.,
1240 Jöckel, P., Jurkat-Witschas, T., Voigt, C., Zahn, A., and Ziereis, H.: Dynamics and
1241 composition of the Asian summer monsoon anticyclone, Atmos. Chem. Phys., 18, 5655-
1242 5675, https://doi.org/10.5194/acp-18-5655-2018, 2018.
1243 Hossaini, R., Chipperfield, M., Montzka, M. P., Rap, S. A., Dhomse, S., and Feng, W.:
1244 Efficiency of short-lived halogens at influencing climate through depletion of stratopsheric
1245 ozone, Nature Geoscience, 8, 186–190, https://doi.org/10.1038/ngeo2363, 2015.
1246 Hoskins, B. J., and Rodwell, M. J.: A model of the Asian summer monsoon, I: The global
1247 scale, J. Atmos. Sci., 52, 1329–1340, 1995.
1248 Highwood, E. J. and Hoskins, B. J.: The tropical tropopause, Q. J. Roy. Meteor.Soc., 124,
1249 1579–1604, 1998.
1250 Houze, R. A., Wilton, D. C., and Smull, B. F.: Monsoon convection in the Himalayan region
1251 as seen by the TRMM 345 Precipitation Radar, Q. J. Roy. Meteor. Soc., 133, 1389-1411,
1252 10.1002/qj.106, 2007.
1253 Hu, Y. and Pan, L.: Arctic stratospheric winter warming forced by observed SSTs, Geophys.
1254 Res. Lett., 36, L11707, doi:10.1029/2009GL037832, 2009.

Kishore, P., Ratnam, M. V., Namboothiri, S., Velicogna, I., Basha, G., Jiang, J., Igarashi, K., Rao, S., and Sivakumar, V.: Global (50◦ S–50◦ N) distribution of water vapor observed by COSMIC GPS RO: Comparison with GPS radiosonde, NCEP, ERAInterim, and JRA-25 reanalysis data sets, J. Atmos. Sol.-Terr. Phy., 73, 1849–1860, doi:10.1016/j.jastp.2011.04.017, 2011.

Kishore, P., Jyothi, S., Basha, G., Rao, S.V.B., Rajeevan, M., Velicogna, I., and Sutterley, T.C.: Precipitation climatology over India: validation with observations and reanalysis datasets and spatial trends. ClimDyn 121. doi: 10.1007/s00382-015-2597-y, 2015.

Kishore, P., Basha, G., VenkatRatnam, M., Velicogna, I., Ouarda, T. B. M. J., and Narayana Rao, D.: Evaluating CMIP5 models using GPS radio occultation COSMIC temperature in UTLS region during 2006–2013: twenty-first century projection and trends, Clim. Dynam., 47, 3253–3270, https://doi.org/10.1007/s00382- 016-3024-8, 2016.

Kalnay, E., Kanamitsu, M., Kistler, R., Collins, W., Deaven, D., Gandin, L., Iredell, M., Saha, D., White, G., Woollen, J., Zhu, Y., Chelliah, M., Ebisuzaki, W., Higgins, W., Janowiak, J., Mo, K.C., Ropelewski, C., Wang, J., Leetma, A., Reynolds, R., and Dennis, J.: The NCEP/NCAR 40-years reanalysis project. Bull. Am. Meteorol. Soc. 77, 437–472. 1996.

Kursinski, E. R., Hajj, G. A., Schofield, J. T., Linfield, R. P., and Hardy, K. R.: Observing Earth's atmosphere with radio occultation measurements using the Global Positioning System, J. Geophys. Res.-Atmos., 102, 23429–23465, 1997.

Kunze, M., Braesicke, P., Langematz, U., and Stiller, G.: Interannual variability of the boreal summer tropical UTLS in observations and CCMVal-2 simulations, Atmos. Chem. Phys., 16, 8695-8714, https://doi.org/10.5194/acp-16-8695-2016, 2016.

Lau, W.K.M., Cheng, Y., and Li, Z.: Origin, maintenance and variability of the Asian Tropopause Aerosol Layer (ATAL): Roles of monsoon dynamics. Sci. Rep. 2018, 8, 3960.

Deleted: 10.1007/s00382-015-2597-y

McPhaden, M. J., Zebiak, S. E., and Glantz M. H. ENSO as an integrating concept in earth science, Science, 314, 1740–1745, 2006.

Medina, S., Houze, R. A., Kumar, A., and Niyogi, D.: Summer monsoon convection in the Himalayan region: terrain and land cover effects, Q. J. Roy. Meteor.Soc., 136, 593-616, 10.1002/qj.601, 2010.

Narendra Reddy, N., Venkat Ratnam, M., Basha, G., and Ravikiran, V.: Cloud vertical structure over a tropical station obtained using long-term high-resolution radiosonde measurements, Atmos. Chem. Phys., 18, 11709–11727, https://doi.org/10.5194/acp-18-11709-2018, 2018.

Pai, D.S., Sridhar, L., and Ramesh Kumar, M.R.: Active and break events of Indian summer monsoon during 1901-2014. ClimDyn 46, 3921– 3939. https://doi.org/10.1007/s00382-015-2813-9, 2016.

Pan, L. L., Honomichl, S. B., Kinnison, D. E., Abalos, M., Randel, W. J., Bergman, J. W., and Bian, J.: Transport of chemical tracers from the boundary layer to stratosphere associated with the dynamics of the Asian summer monsoon, J. Geophys. Res. Atmos., 121, 14159-14174, 10.1002/2016JD025616, 2016.

Park, M., Randel, W. J., Gettleman, A., Massie, S. T., and Jiang, J. H.: Transport above the Asian summer monsoon anticyclone inferred from Aura Microwave Limb Sounder tracers, J. Geophys. Res., 112, D16309, https://doi.org/10.1029/2006JD008294, 2007.

Rajeevan, M., Gadgil, S., and Bhate, J.: Active and break spells of the Indian summer monsoon, J. Earth Syst. Sci., 119, 229–247, doi:10.1007/s12040-010-0019-4, 2010.

Randel, W. J., and Park, M.: Deep convective influence on the Asian summer monsoon anticyclone and associated tracer variability observed with Atmospheric Infrared Sounder (AIRS), J. Geophys. Res., 111, D12314, https://doi.org/10.1029/2005JD006490, 2006

Formatted: Indent: Left: 0", First line: 0"

Formatted: Indent: Left: 0", First line: 0.2"

Formatted: Font color: Text 1

Deleted: 10.1007/s12040-010-0019-4

1306 Rao, D. N., Ratnam, M. V., Mehta, S., Nath, D., Ghouse Basha, S., Jagannadha Rao, V. V.
1307 M., Krishna Murthy, B. V., Tsuda, T., and Nakamura, K.: Validation of the COSMIC
1308 radio occultation data over Gadanki (13.48 N, 79.2 E): A tropical region, Terr. Atmos.
1309 Ocean. Sci., 20, 59–70, doi:10.3319/TAO.2008.01.23.01(F3C), 2009.
1310 Ratnam, M. V., Sunilkumar, S., Parameswaran, K., Murthy, B. K., Ramkumar, G., Rajeev,
1311 K., Basha, G., Babu, S. R., Muhsin, M., and Mishra, M. K.: Tropical tropopause dynamics
1312 (TTD) campaigns over Indian region: An overview, J. Atmos. Sol.-Terr. Phy., 121, 229–
1313 239, 2014
1314 RavindraBabu, S., VenkatRatnam, M., Basha, G., Krishnamurthy, B. V., and
1315 Venkateswararao, B.: Effect of tropical cyclones on the tropical tropopause parameters
1316 observed using COSMIC GPS RO data, Atmos. Chem. Phys., 15, 10239–10249,
1317 doi:10.5194/acp-15-10239-2015, 2015.
1318 Ravindrababu, S., Ratnam, M.V., Basha, G., Liou, Y.-A., Reddy, N.N.: Large Anomalies in
1319 the Tropical Upper Troposphere Lower Stratosphere (UTLS) Trace Gases Observed
1320 during the Extreme 2015–16 El Niño Event by Using Satellite Measurements. *Remote*
1321 *Sens.* 2019, *11*(6), 687; https://doi.org/10.3390/rs11060687, 2019.
1322 Riese, M., Ploeger, F., Rap, A., Vogel, B., Konopka, P., Dameris, M., and Forster, P.: Impact
1323 of uncertainties in atmospheric mixing on simulated UTLS composition and related
1324 radiative effects, J. Geophys. Res., 117, D16305, https://doi.org/10.1029/2012JD017751,
1325 2012.
1326 Santee, M. L., Manney, G. L., Livesey, N. J., Schwartz, M. J., Neu, J. L., and Read, W. G.: A
1327 comprehensive overview of the climatological composition of the Asian summer monsoon
1328 anticyclone based on 10 years of Aura Microwave Limb Sounder measurements, J.
1329 Geophys. Res.-Atmos., 122, 5491– 5514, https://doi.org/10.1002/2016JD026408, 2017

1330 Schreiner, W., Rocken, C., Sokolovskiy, S., Syndergaard, S., and Hunt, D.: Estimates of the
1331 precision of GPS radio occultations from the COSMIC/FORMOSAT-3 mission, Geophys.
1332 Res. Lett., 34, L04808, doi:10.1029/2006GL027557, 2007.
1333 Sokolovskiy, S. V., Kuo, Y.-H., Rocken, C., Schreiner, W. S., Hunt, D., and Anthes, R. A.:
1334 Monitoring the atmospheric boundary layer by GPS radio occultation signals recorded in
1335 the open-loop mode, Geophys. Res. Lett., 33, L12813, doi:10.1029/2006GL025955, 2006.
1336 Solomon, S., Rosenlof, K., Portmann, R., Daniel, J., Davis, S., Sanford, T., and Plattner, G.-
1337 K.: Contributions of stratospheric water vapor to 5 decadal changes in the rate of global
1338 warming, Science, 327, 1219–1223, https://doi.org/10.1126/science.1182488, 2010
1339 Tissier, A.-S., and Legras, B.: Convective sources of trajectories traversing the tropical
1340 tropopause layer, Atmos. Chem. Phys., 16, 3383–3398, doi:10.5194/acp-16-3383-2016,
1341 2016.
1342 Trenberth, K. E.: Recent observed interdecadal climate changes in the Northern Hemisphere,
1343 B. Am. Meteorol. Soc., 71, 988–993, doi:10.1175/1520-0477(1990)0712.0.CO;2, 1990.
1344 Vernier, J. P., Fairlie, T. D., Natarajan, M.,Wienhold, F. G., Bian, J., Martinsson, B. G.,
1345 Crumeyrolle, S., Thomason, L.W., and Bedka, K. M.: Increase in upper tropospheric and
1346 lower stratospheric aerosol levels and its potential connection with Asian pollution, J.
1347 Geophys. Res., https://doi.org/10.1002/2014JD022372, 2015
1348 Vogel, B., Günther, G., Müller, R., Grooß, J.-U., Afchine, A., Bozem, H., Hoor, P., Krämer,
1349 M., Müller, S., Riese, M., Rolf, C., Spelten, N., Stiller, G. P., Ungermann, J., and Zahn,
1350 A.: Long-range transport pathways of tropospheric source gases originating in Asia into
1351 the northern lower stratosphere during the Asian monsoon season 2012, Atmos. Chem.
1352 Phys., 16, 15 301–15 325, https://doi.org/10.5194/acp-16-15301-2016, 2016.
1353 Vogel, B., Günther, G., Müller, R., Grooß, J.-U., and Riese, M.: Impact of different Asian
1354 source regions on the composition of the Asian monsoon anticyclone and of the

extratropical lowermost stratosphere, Atmos. Chem. Phys., 15, 13 699–13 716, https://doi.org/10.5194/acp15-13699-2015, http://www.atmos-chem-phys.net/15/13699/2015/, 2015.

Wickert, J., Reigber, C., Beyerle, G., Konig, R., Marquardt, C., Schmidt, T., Grunwaldt, L., Galas, R., Meehan, T. K., Melbourne, W. G., and Hocke, K.: Atmosphere sounding by GPS radio occultation: First results from CHAMP, Geophys. Res. Lett., 28, 3263–3266, 2001.

Xie, F., Li, J., Tian, W., Feng, J., and Huo, Y.: Signals of El Niño Modoki in the tropical tropopause layer and stratosphere, Atmos. Chem. Phys., 12, 5259-5273, https://doi.org/10.5194/acp-12-5259-2012, 2012.

Yan, R.-C., Bian, J.-C., and Fan, Q.-J.: The impact of the South Asia high bimodality on the chemical composition of the upper troposphere and lower stratosphere, Atmos. Ocean. Sci. Lett., 4, 229–234, 2011.

Yuan, C., Lau, W. K. M., Li, Z., and Cribb, M.: Relationship between Asian monsoon strength and transport of surface aerosols to the Asian Tropopause Aerosol Layer (ATAL): interannual variability and decadal changes, Atmos. Chem. Phys., 19, 1901-1913, https://doi.org/10.5194/acp-19-1901-2019, 2019.

Zhang, Q., Wu, G., and Qian, Y.: The Bimodality of the 100 hPa South Asia High and its Relationship to the Climate Anomaly over East Asia in summer, J. Meteorol. Soc. Jpn., 80, 733–744, 2002.

Zubiaurre, I., and Calvo, N.: The El Nino–Southern Oscillation (ENSO) Modoki signal in the stratosphere, J. Geophys. Res., 117, D04104, doi:10.1029/2011JD016690, 2012.

Deleted: https://doi.org/10.5194/acp1 13699-2015

Deleted: ¶ F

Figures

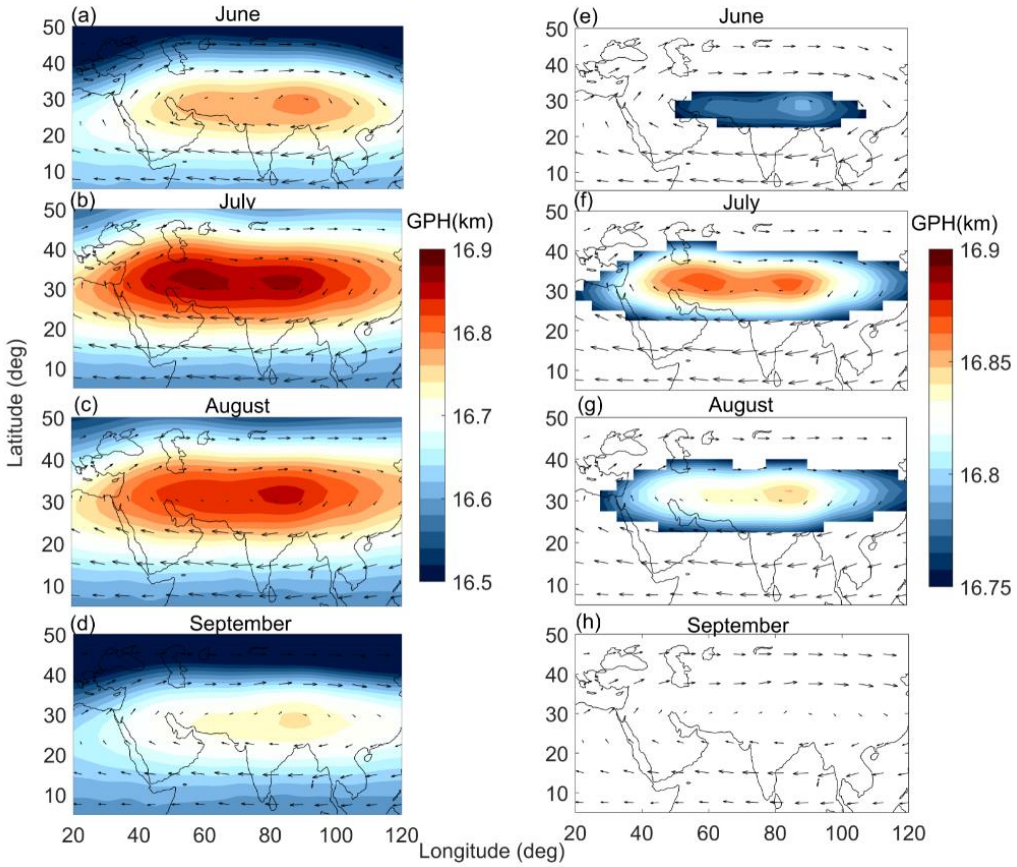

Figure 1. Spatial distribution of Geopotential Height (GPH) and wind vectors at 100 hPa during (a) June, (b), July, (c) August and (d) September from NCEP reanalysis data averaged from the year 1951-2016. The core of the anticyclone region was chosen based on the GPH values ranging from 16.75 to 16.9 km. The spatial extent and magnitude of the anticyclone after applying the GPH criteria for (e) June, (f) July, (g) August and (h), September.

Deleted: 1948

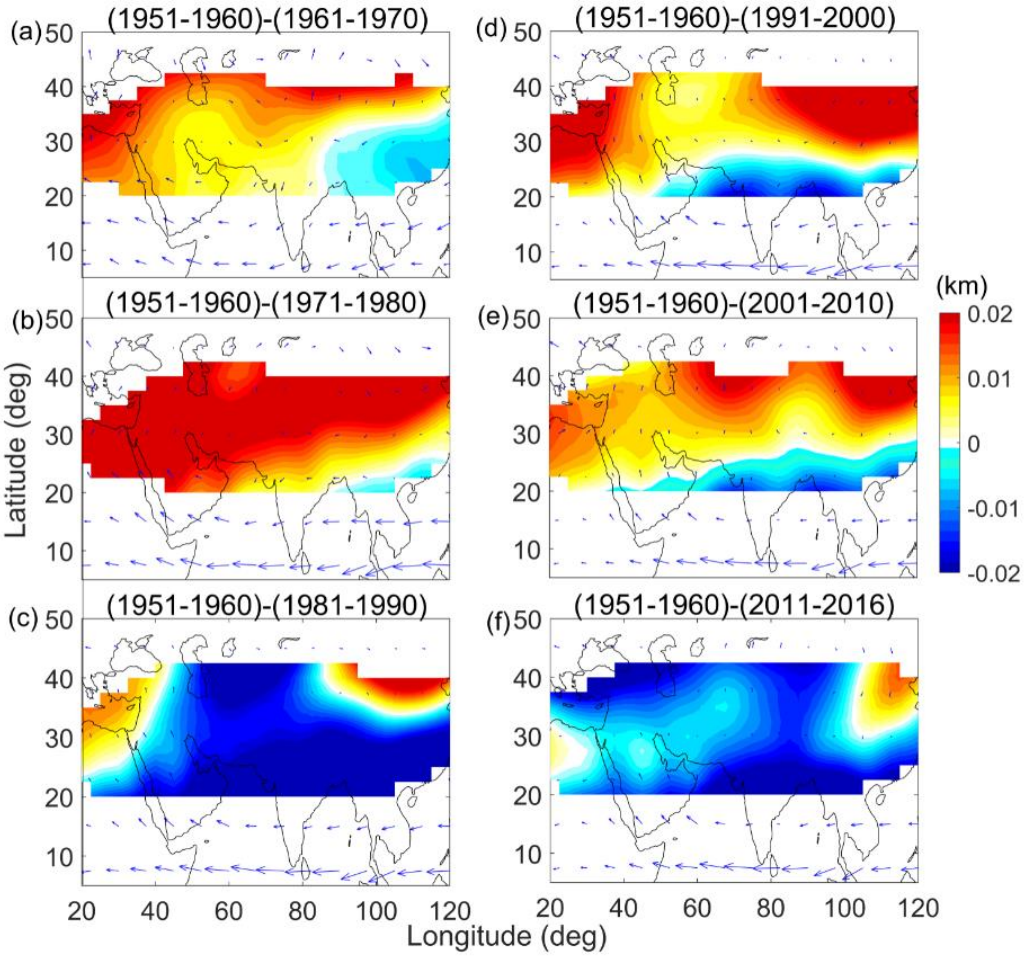

Figure 2. Decadal variation of anticyclone obtained from GPH and wind vectors with reference to 1951-1960 period.

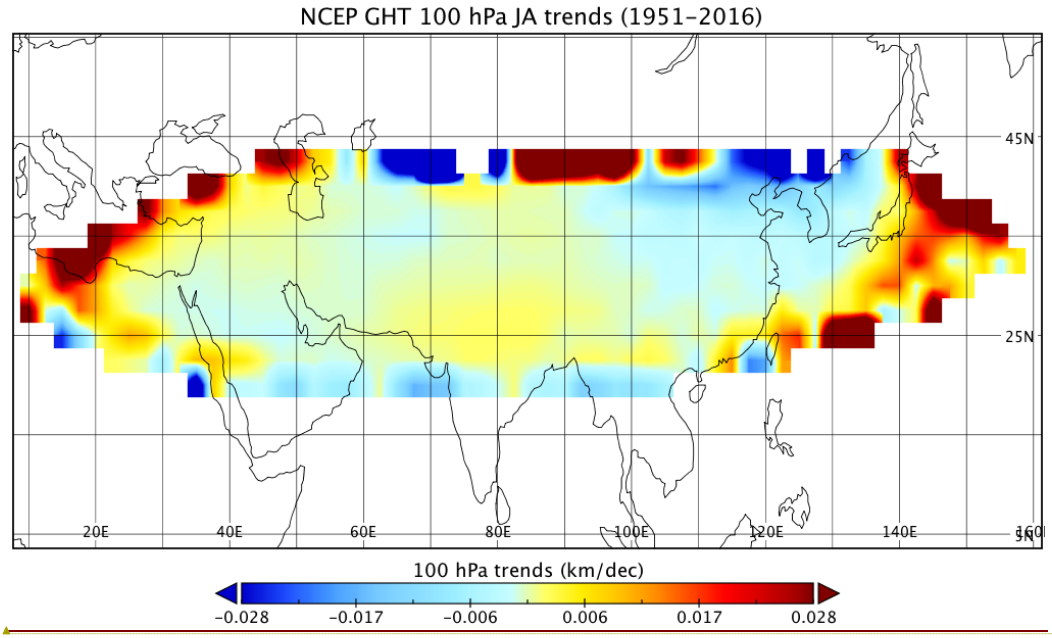

Figure 3. Spatial trend analysis obtained using robust regression analysis at 95% confidence interval.

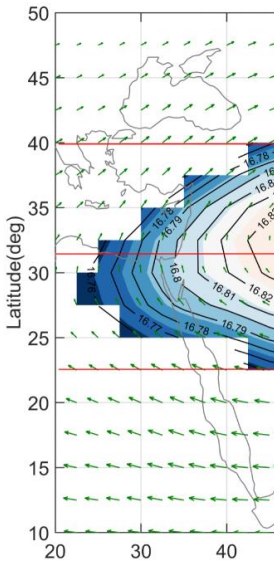

Moved down [2]: Figure 3. (a) Spa trend analysis obtained using robust regression analysis at 95% confidence interval.

Deleted: <*object*>

Formatted: Font color: Black

Formatted: Font color: Black

Deleted: ¶
¶
¶
¶

Moved down [1]: Figure 4.The climatological distribution of GPH (16. to 16.9 km) and wind vectors averaged during July and August from NCEP reanalysis data along with contour lines 100 hPa. The anticyclone region is furt divided in to 4 sectors based on peak values of GPH. The GPH values peak centres at 32.5° N in latitude and 70°E i longitude. The sectors are further divid in to South-East (SE) (22.5°N-32.5°N), North-East (NE) (32.5°N-40°N) in longitude band 70°E-120°E, South-Wes (SW) (22.5°N-32.5°N), and North-Wes (NW) (32.5°N-40°N) at 20°E-70°E longitude range.

Deleted:

Moved (insertion) [2]

Deleted: (a)

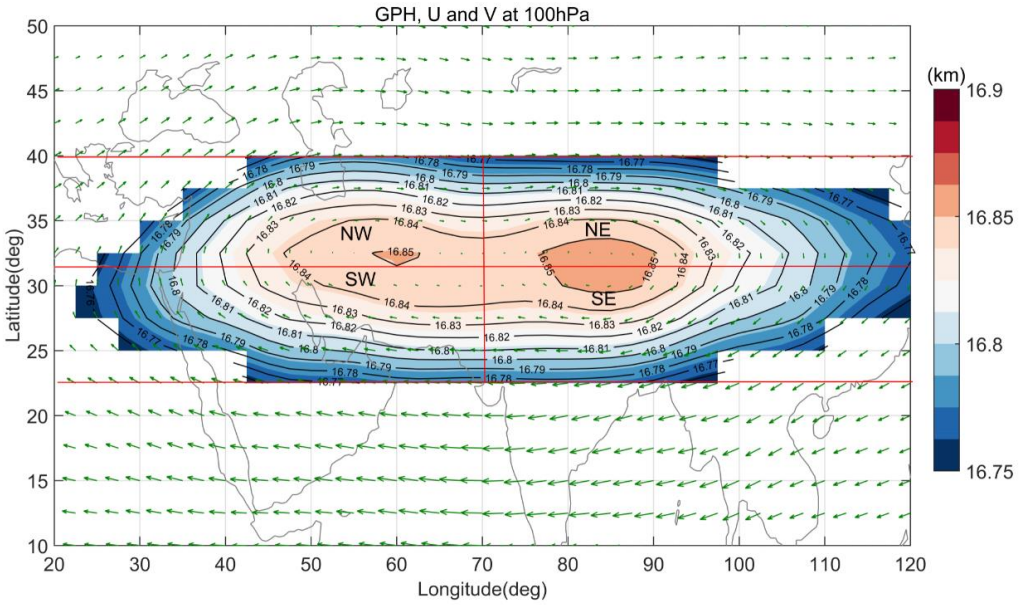

Figure 4.The climatological distribution of GPH (16.75 to 16.9 km) and wind vectors averaged during July and August from NCEP reanalysis data along with contour lines at 100 hPa from 1951-2016. The anticyclone region is further divided in to 4 sectors based on peak values of GPH. The GPH values peak centres at 32.5°N in latitude and 70°E in longitude. The sectors are further divided in to South-East (SE) (22.5°N-32.5°N), North-East (NE) (32.5°N-40°N) in longitude band 70°E-120°E, South-West (SW) (22.5°N-32.5°N), and North-West (NW) (32.5°N-40°N) at 20°E-70°E longitude range.

Moved (insertion) [1]

Deleted:

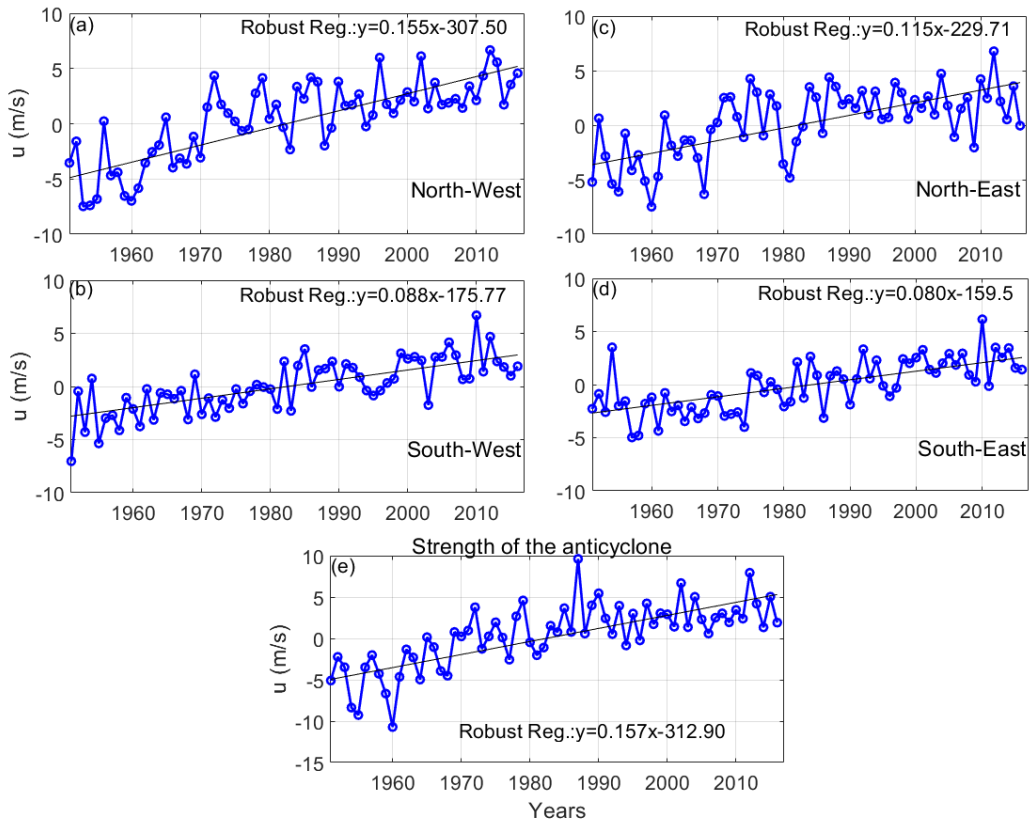

Figure 5.Time series of zonal wind anomalies estimated for (a) North-West, (b) South-West, (c) North-East and (d) South-East sectors of ASMA. The trend analysis was performed at 95% confidence interval by using robust regression analysis. (e) The strength of the anticyclone was estimated from the zonal wind difference between (30^{o}N-40^{o}N)-(10^{o}N-20^{o}N) in the longitude band of 50^{o}E-90^{o}E.

Deleted: ¶

Deleted: anomalies in

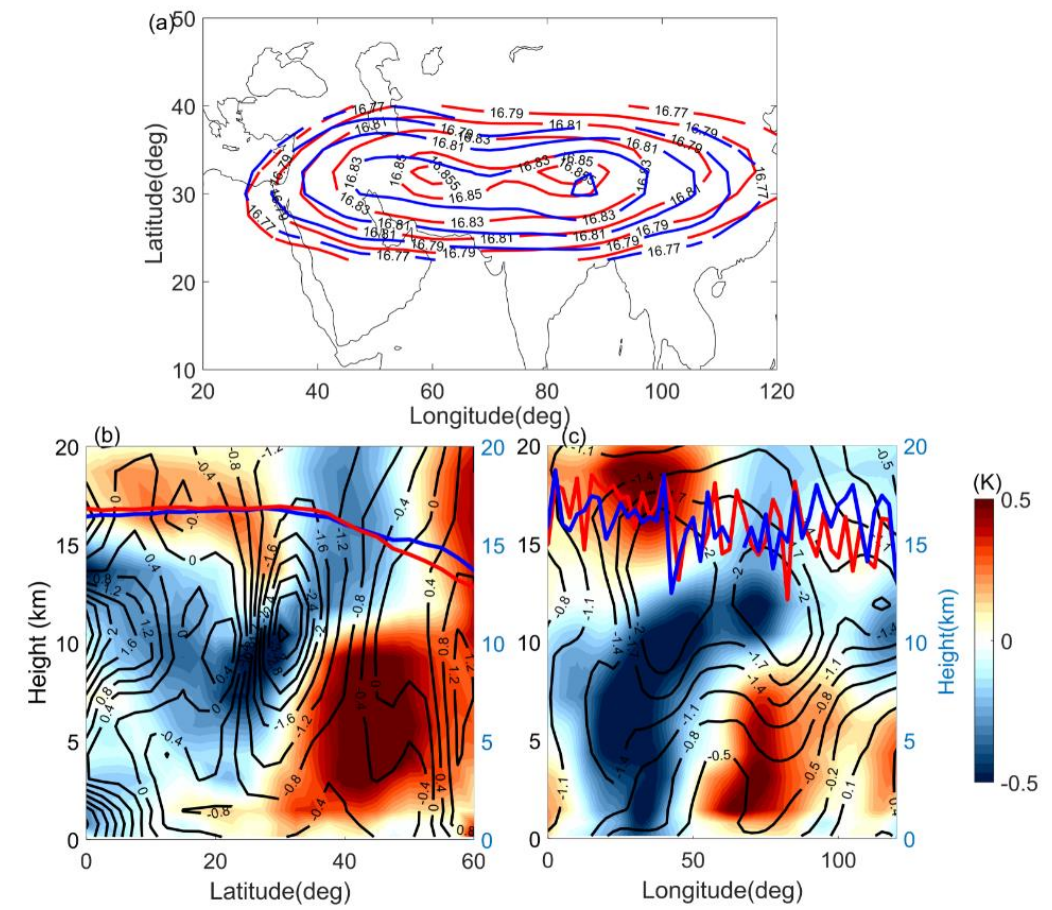

Figure 6. (a) ASMA variability during active and break phases of Indian monsoon obtained from GPH at 100 hPa. Red line indicates the active and blue line for break phase of Indian monsoon. (b) Latitude-altitude cross-section of temperature (colour shaded, K) and zonal wind anomalies (contour lines, m/s) which are estimated from difference between active and break phases of Indian Monsoon in the longitude band of 80°E-90°E. (c) Longitude-altitude cross-section of temperature and wind anomalies averaged between 30°N-40°N. The red and blue lines in Figure 6b & 6c denotes the tropopause altitude during active and break spells of Indian monsoon estimated using GNSS RO data, respectively.

Deleted:

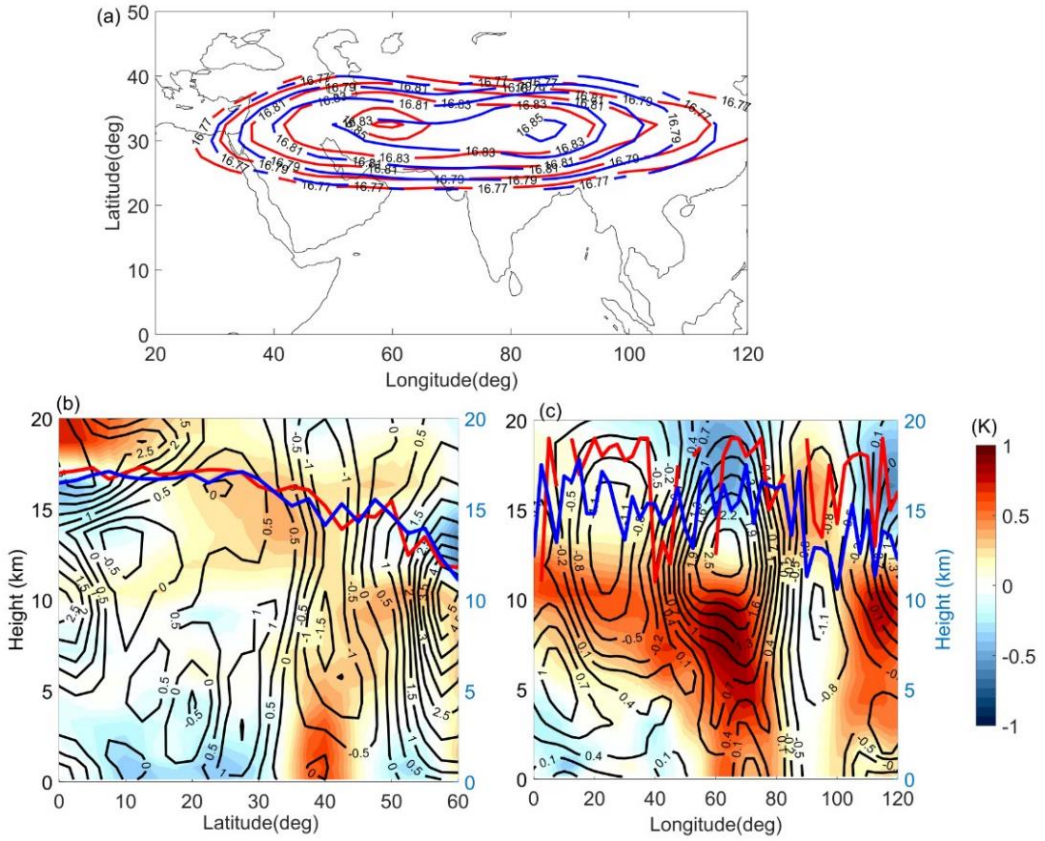

Figure 7. (a) ASMA variability obtained from GPH at 100hPa during strong and weak monsoon years calculated based on high resolution rainfall data in band of 5°N-30°N, 70°N-95°E grid. Red line indicates the strong and blue line for weak monsoon years. (b) Latitude-altitude cross-section of temperature (colour shaded, K) and zonal wind anomalies (contour lines, m/s) which are estimated from difference between strong and weak monsoon years in the longitude band of 80^{o}E-90^{o}E. (c) Longitude-altitude cross-section of temperature and wind anomalies averaged between 30^{o}N-40^{o}N. Red and blue lines in Figure 7b & 7c denote the tropopause altitude during strong and weak monsoon years estimated using GNSS RO data, respectively.

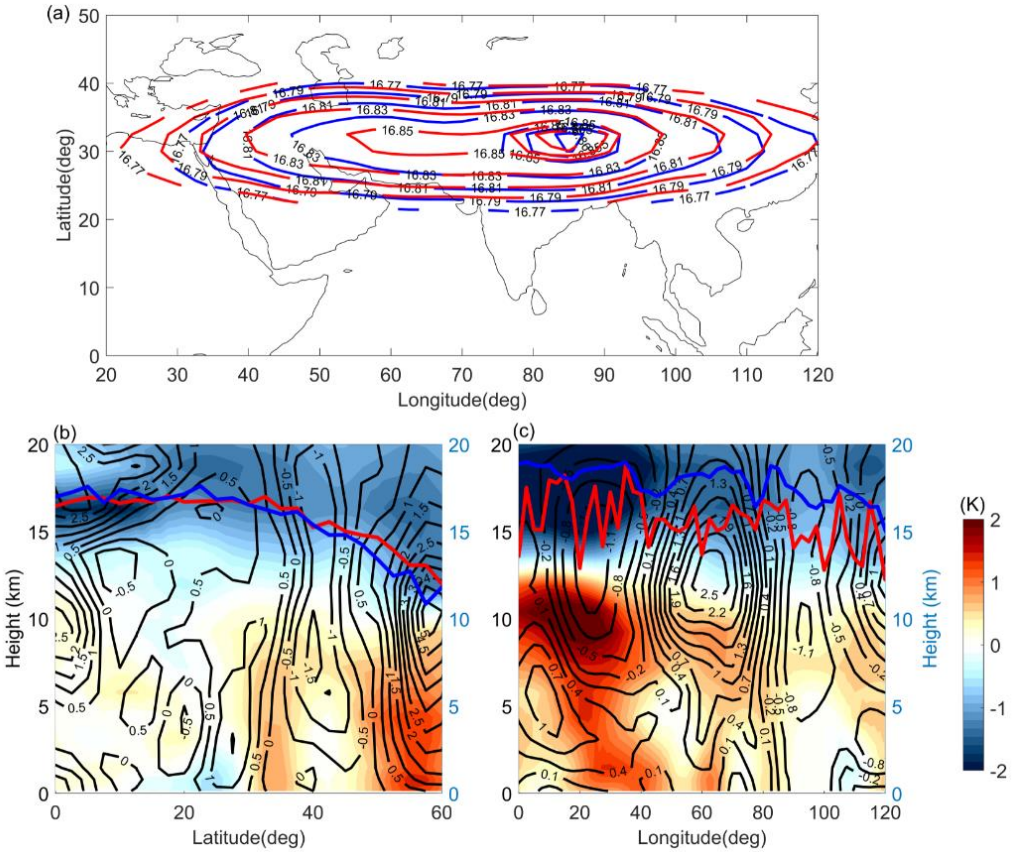

Figure 8. (a) ASMA variability obtained from GPH at 100 hPa during strong La Niño and El Niño years. Red and blue lines indicate the La Niño and El Niño years. (b) Latitude-altitude cross-section of temperature (colour shaded, K) and zonal wind anomalies (contour lines, m/s) which are estimated from difference between La Niño and El Niño years in the longitude band of 80°E-90°E. (c) Longitude-altitude cross-section of temperature and zonal wind anomalies averaged between 30°N-40°N. The red and blue lines in Figure 8b & 8c denote the tropopause altitude during La Niño and El Niño years estimated from GNSS RO data, respectively.